NEUTRON HOLE DISTRIBUTIONS IN ^{111,115,119}Sn AS OBSERVED IN THE (^{3}He,α) REACTION

E.Gerlic, G.Berrier-Ronsin, G.Duhamel, S.Galès, E.Hourani, H.Langevin-Joliot, M.Vergnes and J.Van de Wiele

IPNO-PHN-79-20

université paris sud
INSTITUT DE PHYSIQUE NUCLEAIRE
BP. N° 1 91406 - ORSAY TEL. 941.51.10
laboratoire associé à l'IN2 P3

NEUTRON HOLE DISTRIBUTIONS IN ^{111,115,119}Sn AS OBSERVED IN THE (^{3}He,α) REACTION

E.Gerlic, G.Berrier-Ronsin, G.Duhamel, S.Galès, E.Hourani,
H.Langevin-Joliot, M.Vergnes and J.Van de Wiele

Institut de Physique Nucléaire, BP n°1, 91406 Orsay, France

The energy spectra of residual ^{111,115,119}Sn nuclei have been studied with 38 keV resolution, up to excitation energies of the order of 16 MeV, using the (^{3}He,α) reaction at 39 MeV. Complete angular distributions have been obtained for the ^{116}Sn(^{3}He,α)^{115}Sn reaction ; two angles were measured for the other isotopes. Several new levels or groups are observed up to ∿3.5 MeV in the three isotopes, due to the momentum matching conditions. Spectroscopic factors are determined for all observed levels up to 3.71 MeV in ^{115}Sn and for the low-lying strongly populated levels with known J^π in ^{111,119}Sn. The fragmentation of the $\ell = 4$, 5 valence hole strengths and the excitation of levels with anomalous spins and parities in the intermediate energy region in ^{115}Sn are discussed in terms of weak coupling and two step coupled channels calculations. The fine structure previously reported for the $^1g_{9/2}$ hole orbital in ^{115}Sn is clearly confirmed and enhanced in the present experiment. The fragmentation of this orbital is observed for the first time in ^{111}Sn, between 3.4 and 5.2 MeV and in ^{119}Sn, though to a lesser extent, between 3.8 and 6.5 MeV. In the fine structure region the $^1g_{9/2}$ hole strength is found to decrease from 62% to 43% and 28% in respectively ^{111}Sn, ^{115}Sn and ^{119}Sn; theoretical calculations do not explain these experimental strengths and fragmentations. The first $9/2^+$, $1/2^-$, $3/2^-$ IAS are identified in ^{111}Sn.

Previously unreported, weakly populated IAS are also found in ^{115}Sn and ^{119}Sn. The energies and widths are measured. The spectroscopic factors and isospin splitting of these states are discussed in the framework of the Lane coupled channels formalism for the neutron form factor.

NUCLEAR REACTIONS ^{112,116,120}Sn(^{3}He,α) E = 39 MeV ; measured $\sigma(E_{\alpha},\theta)$ ^{111,115,119}Sn deduced levels, E_x, ℓ, $(J)^{\pi}$, C^2S ; zero-range DWBA and two-step process analysis ; inner shells and isobaric analog states analysis : enriched targets, magnetic spectrometer.

NUCLEAR STRUCTURE unified model calculations

I. Introduction

In the last few years, neutron pick-up experiments on the tin isotopes have been carried out using the reactions : (d,t) at 23 MeV [1,2] and 52 MeV [3], (p,d) at 20 MeV [4] and 52 MeV [5], (^{3}He,α) at 89 MeV [5], 120 MeV [6] and 205 MeV [7]. With the exception of Ref.4, these studies concentrated on deeply bound hole states and in some cases on their corresponding isobaric analog states (IAS). The (^{3}He,α) studies were performed with rather poor energy resolution (190-400 keV). The resent high resolution study of the ^{116}Sn(d,t) ^{115}Sn reaction at 23 MeV [1] demonstrated an underlying fine structure between 4 and 6 MeV excitation energy, with both ℓ=4 and ℓ=1 inner hole components. This reaction also proved useful for the determination of a number of transitions with small ℓ values at lower excitation energy[2].

We present in this paper a rather extensive study of the (^{3}He,α) reaction at 39 MeV incident energy on ^{116}Sn, and a cursory investigation at two angles of this reaction on ^{112}Sn and ^{120}Sn. The selectivity of the (^{3}He,α) reaction for high angular momentum, together with the adequate energy resolution (38 keV), were used in order to investigate the fragmentation of $1g_{7/2}$ and $1h_{11/2}$ valence orbitals as well as that of the $1g_{9/2}$ inner orbital. The spectra of the residual nuclei were investigated up to $\sim$16 MeV excitation energy.

After a short description of the experimental procedure (Sec.II), we present in Sec.III the analysis of the data, involving zero range one step DWBA calculations. Two-step processes, in the framework of the weak coupling model, will be considered in the discussion of neutron hole states fragmentation at intermediate excitation energies, i.e. from $\sim$1 MeV up to $\sim$3.7 MeV (Sec.IV). Rather sparse spectroscopic information exists in that region, especially in the case of ^{111}Sn. In Section V the observed fragmentation of the

$1g_{9/2}$, $T_<$, inner hole strength in the Sn isotopes around 5 MeV excitation energy, will be discussed. In Section VI, data and analysis of the $T_>$ ($1g_{9/2}$, $2p_{3/2}$, $2p_{1/2}$ and $1f_{5/2}$) inner hole components will be presented.

II. Experimental procedure.

The $^{112,116,120}Sn(^3He,\alpha)$ reactions were studied at 39 MeV incident energy using the ^3He beam delivered by the Orsay MP Tandem accelerator. The outgoing α particles were detected in 8 position sensitive detectors (PSD) in the focal plane of the split pole magnetic spectrometer. The solid angle of the spectrometer was 1.7 msr. The targets consisted of self supporting metal foils of ^{112}Sn (420 $\mu g/cm^2$, 83.64% enrichment), ^{116}Sn (290 $\mu g/cm^2$, 95.74% enrichment) and ^{120}Sn (380 $\mu g/cm^2$, 98.4% enrichment), prepared by vacuum evaporation. An overall energy resolution of 38 keV was achieved. The alpha particle spectra obtained for the three targets are presented in Fig. 1 and 2 for the low-lying states ($E_x < 4$ MeV). The excitation energy range from ~ 3 to ~ 16 MeV, where the $T_<$ and $T_>$ components of inner hole states are observed, is displayed for the three isotopes in Fig.3a,b,c.

The absolute cross sections were determined by measuring the thicknesses of the targets using an α gauge. The beam current was measured in a Faraday cup. The error in the absolute cross-section scales is estimated to be of the order of $\pm$ 13%. The excitation energies of the observed levels have been determined from calibration of the PSD using both a Th C α source and reaction α particles. The uncertainties on the excitation energies are estimated to be of the order of $\pm$ 8 keV for strong transitions up to 6 MeV and about $\pm$ 15 keV for weaker or complex groups for $E_x > 6$ MeV. Angular distributions have been measured from 4° to 22°, typically by 2° steps, in the case of the $^{116}Sn(^3He,\alpha)^{115}Sn$ reaction. The spectra of the $^{112}Sn(^3He,\alpha)^{111}Sn$ and

$^{120}Sn(^{3}He,\alpha)^{119}Sn$ reactions have been measured at $\theta_{lab}=4°$ and 12° for comparison. The most forward angles could only be measured, with reasonable beam intensity, by removing the defining slits at the entrance of the scattering chamber.

In Fig.1,2, one can notice that, above $\sim$2 MeV, the spectrum no longer consists of well separated levels. Peaks or groups of peaks are however clearly identified at most angles and angular distributions could be obtained for ^{115}Sn by dividing the spectra into adjacent slices carefully chosen in order to be consistent with our previous (d,t) work. The experimental angular distributions,obtained using such a procedure,were found to be rather simple, and could in most cases be fitted by a dominant ℓ transfer, due to the high selectivity for large ℓ values of the $(^{3}He,\alpha)$ reaction.

III. Distorted waves analysis, optical potential parameters.

The experimental angular distributions obtained in the study of the $^{116}Sn(^{3}He,\alpha)^{115}Sn$ reaction were analysed first in the framework of the DWBA theory of direct reactions. The calculations of the theoretical curves were made using the code DWUCK[8] with the zero range, local approximation (ZRL).

A number of different sets of ^{3}He and α optical potentials (deep families), taken from the compilation of Perey et al.[9] and/or from some more recent elastic scattering and transfer reaction studies[10], were used in order to reproduce the strongest transitions at $E_x = 614$ keV, $7/2^+ - E_x = 714$ keV, $11/2^-$ and $E_x = 985$ keV, $5/2^+$, in ^{115}Sn. No significant differences were observed in the shapes of the angular distributions or in the resulting relative cross-sections for different ℓ values. However, depending on the choice of the optical parameters, the absolute cross-sections were found to show differences of the order of $\pm$ 15% for a given level.

Table I gives the adopted sets of parameters[10,11] for the ^{3}He and α channels. The same potentials were used to extract spectroscopic factors for the well known low-lying levels in ^{111,119}Sn. The normalisation constant N was taken equal to 23 in the whole analysis.

A more refined analysis, taking into account two-step processes for some levels in ^{115}Sn or using a Lane form factor for $T_>$ states, will be discussed in Sec.IV and VI.

IV. Fragmentation in the low and intermediate energy region ($0. < E_x < \sim 3.7$ MeV)

A. DWBA analysis of the ^{116}Sn(^{3}He,α)^{115}Sn reaction

The measured cross sections for the first low-lying levels ($1/2^+$, $3/2^+$, $7/2^+$, $11/2^-$, $5/2^+$) in ^{115}Sn clearly demonstrate the selectivity of this reaction for high spin states (see Fig.1,4). Moreover, the transitions : ℓ=0 to the E_x = 0.0 and 1964 keV levels, strong in the (d,t) spectrum, are barely visible in the (^{3}He,α) spectrum (see Fig.1,4 and Table II).

Above 2.6 MeV excitation energy in ^{115}Sn the observed cross section remains large in the (^{3}He,α) spectrum (see Fig.1) while in the (d,t) spectrum the cross section is much smaller in the same excitation energy range. This observation suggests that high ℓ components are present in this part of the spectrum.

The experimental angular distributions are displayed in Fig.4 and 5. As expected for the (^{3}He,α) reaction, they are not very characteristic of the transfered angular momentum, especially for two transfers differing by only one unit of ℓ (ℓ=4 or 5 for example). However, a careful comparison between the experimental data and theoretical DWBA curves allows in most cases an unique ℓ assignment for the observed levels in ^{115}Sn. In addition, compa-

rison has been made with the $^{116}Sn(d,t)^{115}Sn$ results, in order to clarify any ambiguous assignment due to the contribution of two different ℓ values within the same complex peak. The deduced spectroscopic information is presented in Table II together with the C^2S values from the $^{116}Sn(d,t)^{115}Sn$ study[2]. The main characteristics of the intermediate energy region (E_x = 1 to 3.7 MeV) are the following :

i) The states observed for the first time in the (d,t) experiment[2] with an angular momentum $\ell \geq 3$ are clearly enhanced in the ($^3He,\alpha$) spectrum :

. The 1950 keV state, which dominates this part of the spectrum, has a definite ℓ=5 angular momentum transfer, suggesting $J^\pi = 11/2^-$ from shell model considerations.

. The 2155, 2370 and 3670 keV states have angular distributions in good agreement with an ℓ=4 transfer, leading to spin and parity assignments $J^\pi = 7/2^+$ or $9/2^+$.

. The 2305 and 3290 keV states have an ℓ=3 angular distribution, suggesting spin and parities $J^\pi = 5/2^-$ or $7/2^-$.

ii) In addition, new states are observed in this ($^3He,\alpha$) experiment :

. The 1805 keV state has an angular distribution nicely reproduced by an ℓ=6 transfer.

. The peaks or groups of peaks located respectively at 3070, 3190, 3405 and possibly 3490 keV are populated through an ℓ=5 transfer. An ℓ=4 component may also contribute to the complex 3070 keV peak, as suggested by the (d,t) analysis.

. A number of weaker transitions are identified as ℓ=4 (E_x = 2487 and 3590 keV), ℓ=5 (E_x = 2890 and 2985 keV), ℓ=6 (E_x = 2860 keV) ; the rather strong 2745 keV transition might also be ℓ=6.

iii) We would like to stress that probable ℓ=3 transitions are observed at $\sim$ 2080 and 2208 keV. In both the (d,t) and (^{3}He,α) studies, these levels are observed as complex peaks and have dominant ℓ=2 contributions in their angular distributions. However, the extracted C^2S values assuming a simple ℓ=2 transfer are much larger in the (^{3}He,α) study than in the (d,t) work. An attempt was made to explain the discrepancies by introducing small contributions from an ℓ=3 angular momentum transfer in the DWBA analysis. The resulting fits to the experimental data assuming ℓ=2+3 mixing are presented in Fig.4 and the deduced C^2S values are listed in Table II. These ℓ=3 contributions are in agreement with the spin assignments (5/2,7/2) for the level at 2207 keV in Madueme's work[12] and with the recent results of Fleming et al.[13] in their study of the ^{115}Sn(p,p')^{115}Sn reaction. In this last experiment, strongly excited levels at E_x = 2090, 2200 and 2310 keV are assigned J^π=5/2$^-$ or 7/2$^-$.

iv) Finally, we note the rather large discrepancy observed between the spectroscopic factors deduced from the (^{3}He,α) and (d,t) reactions, for the unambiguous ℓ=2 transitions populating the levels at E_x = 1280 and 1420 keV (see Table II). The behaviour of the two states, in the two experiments, is obviously different, leading to the observed differences in the C^2S values. As was already pointed out in the previous (d,t) work[2], these levels are respectively the second J^π=3/2$^+$ and J^π=5/2$^+$ levels of ^{115}Sn and are predicted to have wave functions containing very large $|3s_{1/2} \otimes 2^+>$ collective components. This is confirmed by the strong excitation of these levels in the (p,p') experiment of Flemming[13]. The observed anomalies are therefore very probably due to two-step processes in both reactions.

In summary, the intermediate energy region in ^{115}Sn (E_x = 1 to 3.7 MeV) is dominated by a large number of transitions with ℓ = 3, 4, 5 and 6 transfers. In the framework of a simple shell model the observation of such ℓ=6 ($11/2^+$, $13/2^+$)

as well as ℓ=3 ($5/2^-$,$7/2^-$) states at so low an excitation energy is clearly unexpected. It is also quite difficult to explain the presence of "anomalous" negative parity states populated through an ℓ=1 transfer ($1/2^-$,$3/2^-$), strongly enhanced in the (d,t) experiment[2]. The observation, at low excitation energy, of these "anomalous ℓ" states populated with small but non negligible spectroscopic factors ($C^2S < 0.2$) is an indication of the need for a refined description of the low-lying levels of ^{115}Sn. The introduction of a weak-coupling model, already proposed in our previous (d,t) study to explain the fragmentation of the ℓ=2, ($2d_{3/2}$ and $2d_{5/2}$) subshells in ^{115}Sn, could give a quantitative explanation to the fragmentation observed in this excitation energy region for the $\ell > 2$ orbitals in ^{115}Sn.

B. Weak coupling model for ^{115}Sn.

In order to explain the population of "anomalous states" in the intermediate excitation energy region, an unified model calculation has been performed. The quasi hole neutron configurations of valence as well as of inner orbitals are coupled to the quadrupole (2^+) and octupole (3^-) vibration modes of the doubly even ^{116}Sn nucleus. The required formulae involved in these calculations are rather standard and have been reported in detail, for example in Ref.14. The computer code QUPHONON, written by K.Heyde[15], was used to obtain the wave functions of the ^{115}Sn levels based on this model. All combinations up to 3 quadrupole and 2 octupole phonons, with experimental phonon energies $\hbar\omega_2$ = 1.27 MeV and $\hbar\omega_3$ = 2.27 MeV, are introduced in the calculations. The quasi hole neutron valence orbitals outside the N=50 core ($3s_{1/2}$, $2d_{5/2}$, $2d_{3/2}$, $1g_{7/2}$, $1h_{11/2}$) as well as inner neutron hole orbitals ($1g_{9/2}$, $2p_{1/2}$, $2p_{3/2}$, $1f_{5/2}$ and $1f_{7/2}$) were also introduced in the calculations. The valence occupation probabilities V_j^2 were taken as the mean values between those extracted from previous neutron pick-up data[2,3,16] on ^{116}Sn and those from the

present (^{3}He,α) data. This procedure seems to relax somewhat the dependence on momentum mismatch effects in a particular reaction and on reaction mechanisms. The different allowed combinations for a given J^π value, up to an excitation energy of $E_x = 12$ MeV, are taken into account to prevent any effect due to a limited configuration space in the relevant excitation energy region. The coupling strength $\xi_\lambda = \langle r \frac{\partial V}{\partial r} \rangle \beta_\lambda \frac{1}{\hbar\omega_\lambda \sqrt{\pi}}$ is estimated from inelastic scattering or Coulomb excitation measurements, using the currently adopted value of 40-50 MeV for the expression $\langle r \frac{\partial V}{\partial r} \rangle$. The values of ξ_λ as well as the quasi hole energies were considered to some extent as parameters in the analysis in order to reproduce the level sequence of the first well known low-lying levels in ^{115}Sn, where the lowest level of each spin is known to carry the main part (> 75%) of the corresponding measured strength. The largest deviation (465 keV) between any nℓj quasi-hole energy and the experimental excitation energy of the corresponding lowest J^π excited state is found for $2d_{5/2}$, showing a relatively larger fragmentation of this orbital. The resulting values of ξ_2 and ξ_3, quasi-hole energies E_{qp} and occupation probabilities V_j^2 are reported in Table III. The agreement is rather good as shown in Fig.6. The large spectroscopic factors of the first 5 levels below 1 MeV are well reproduced by the unified-model. These theoretical values are defined as $C^2S = (2j+1)\ V_j^2\ C_j^2\ 0^+$ where $C_j 0^+$ is the amplitude of the ℓ_j quasi-hole coupled to the 0^+ ground state core. The first level of each spin has a rather pure single hole character ($C_j 0^+ \geq 0.92$, except for the $5/2_1^+$ level where $C_j 0^+ = 0.84$), leading to very small predicted C^2S values for all the other states located above 1 MeV, in agreement with the general trend experimentally observed.

The introduction of 5 inner orbitals extends our previous unified model calculation in ^{115}Sn where only the $1g_{9/2}$ inner orbital was considered in addition to the 6 valence orbitals. Thus the present calculation predicts in particular that small but significant fractions of the 2p and 1f strengths

are concentrated on a few relatively low-lying (2 to 3 MeV) levels, in agreement with the (d,t) observations and with the predictions of ref.17. We wish to emphasize that these calculations predict large ℓ transitions, populating positive ($7/2^+$ to $11/2^+$) and negative ($5/2^-$ to $11/2^-$) parity states in the intermediate energy region of the (^{3}He,α) spectra. A comparison up to 2.5 MeV is presented in Fig.6.

The general trend of the experimental results (levels excitation energies, spins and parities) is rather well reproduced by the present unified model calculation, with however some discrepancies between theoretical and experimental spectroscopic factors. One notices that two-step pick-up amplitudes may interfere with direct pick-up ones and may thus modify the deduced C^2S for the levels above $\sim$ 1 MeV which have obviously strong collective components.

C. Coupled channels calculations for ^{115}Sn.

Coherent coupled channels calculations for the ^{116}Sn(^{3}He,α)^{115}Sn reaction at 39 MeV were performed with the weak-coupling wave functions discussed in the preceding paragraph, using the code CHUCK[18].

The general features of these calculations, for purely collective states (pure two-step process only), are the following :

i) collective excitation in the α channel plays an important role and has to be taken into account, in addition to the ^{3}He one.

ii) the two inelastic form factors involved in the inelastic (^{3}He,^{3}He') or (α,α') channels were calculated using similar β_R deformation lengths

iii) the angular distribution of a level with total angular momentum J in a multiplet $|n\ell j \otimes 2^+\rangle_J$ is rather similar to that of a direct L,J equivalent pick-up if $J = L + \frac{1}{2}\varepsilon$, when $j = \ell + \frac{1}{2}\varepsilon$ (with $\varepsilon = \pm 1$). On the contrary, the members of the multiplet with $J = L - \frac{1}{2}\varepsilon$ have a typical "bell" shape angular distribution and smaller cross-sections.

In the excitation energy range : $1.5 < E_x < 3.5$ MeV, most of the weak coupling wave functions are a mixture of strong collective components plus a one hole component. These wave functions were used to perform coupled channels calculations : a few typical comparisons between the resulting theoretical angular distributions and the experimental ones are presented in Fig.7. Taking into account the complexity involved in such calculations, the agreement can be considered as acceptable. The new state observed at 1805 keV is well reproduced by the calculations assuming it is the $11/2^+$ member of the $|g_{7/2} \otimes 2^+>$ multiplet. As mentionned in (iii) above, we notice that the pure two step curve is very similar to the $\ell=6$ direct transfer one.

The one hole component generally dominates (due to matching conditions) the population of the other levels although the addition of the two step amplitude changes significantly the predicted cross sections, partly solving the "apparent" discrepancy between predicted and observed C^2S. The spin assignments proposed for the strongest $\ell \geq 3$ "equivalent" direct transitions observed in the present experiment between $\sim$ 1. and $\sim$ 3.7 MeV, are summarized in Table IV and Fig.7.

We wish to draw attention to the observation of some weaker structures between $\sim$ 2.9 MeV and $\sim$ 3.6 MeV, having an $\ell=5$ dominant behaviour. They are in agreement with the weak-coupling picture which predicts several $11/2^-$ states in that region, due to the fragmentation of the $11/2^-$ member of the $|2d_{5/2} \otimes 3^->$ multiplet, by interaction with other multiplets (see Table IV). The wave functions of these states contain a significant $h_{11/2}$ quasi-hole component.

We would like to point out that these calculations also account for the shape and about half of the cross section of the 2600 keV peak, obviously complex in the (^{3}He,α) experiment while observed as a single peak and assi-

gned pure ℓ=1 in the (d,t) experiments[2,3]. The calculations describe this state as the $1/2^-$ member of the $|1g_{7/2} \otimes 3^->$ multiplet, with a quite large ($C_j 0^+ = 0.26$) inner hole component, in agreement with Koeling and Iachello's calculations[17] on the fragmentation of inner orbitals.

In summary, the (^{3}He,α) reaction has revealed or confirmed the observation of new states in the $\sim$ 1.6 MeV to $\sim$ 3.7 MeV excitation energy region of ^{115}Sn ; the population of such states is well reproduced by the weak-coupling model and two-step calculations.

The selectivity of the reaction allows the observation of rather high spin states with strong collective character, which are difficult to observe in (p,d) or (d,t) reactions or even in inelastic scattering, where only the population of states corresponding to the coupling of collective even core states with the $1/2^+$ ground state is strongly enhanced.

We have also shown the necessity of including the inner hole states in the model, in order to explain some "anomalous" spin and parity states lying at low excitation energy. This fragmentation reveals a strong coupling between these inner hole states, lying at rather high excitation energy (> 5 MeV) and the first (2^+,3^-,...) collective states of ^{116}Sn.

D. The ^{112,120}Sn(^{3}He,α)^{111,119}Sn reactions.

The neutron hole distributions in ^{111}Sn and ^{119}Sn were investigated up to $\sim$ 16 MeV excitation energy. The experimental data were recorded at two angles (4° and 12° laboratory angles) for comparison with the ^{115}Sn data. The neutron pick-up data[4,16,19] on these nuclei are rather scarce and, for C^2S informations, the only possible comparison with previous work was with the (p,d) study of Flemming[4], which was however limited to the low-lying levels (up to 655 keV in ^{111}Sn and up to 2.2 MeV in ^{119}Sn). During the writing of the present paper, new (p,d) data[20] at 27.5 MeV incident energy on ^{112}Sn

became available. No (^{3}He,α) experiment has previously been reported on these two nuclei.

Typical energy spectra are given in Fig.2, obviously showing quite different features. This is not surprising in view of the weak-coupling picture described above for ^{115}Sn. The quasi hole valence energies involved vary quite strongly from one isotope to the other (as can be seen from the relative position of the first strongly excited $7/2^+$ and $5/2^+$ states as compared to the $11/2^-$ one). In addition, the evolution, although smoother, of 2^+ and 3^- phonon energies of doubly even Sn isotopes have to be taken into account.

From ∿2. MeV to ∿3.6 MeV, the spectrum of ^{119}Sn appears obviously more complex than the one of ^{111}Sn. A comparison between C^2S values for the first strongly excited low-lying states of ^{111,115,119}Sn is presented in table V, together with the results from previous (p,d) studies[4,20] and with the results of our weak-coupling calculations, extended to ^{111}Sn and ^{119}Sn. The results are now discussed for each isotope, in the framework of this model.

^{111}Sn. Above ∿1. MeV excitation energy, very little is known about this isotope. In the present experiment, from ∿1. to ∿3.5 MeV excitation energy, the spectrum is dominated by previously unobserved strong structures located at 1280, 1470, 2070 and 2320 keV. The peak at 1280 keV is obviously complex and, although it includes the $5/2^+$ state observed at 1320 keV by Cavanagh[19], its important population in the (^{3}He,α) experiment strongly suggests that a new level is populated by an $\ell > 2$ transfer. The first low-lying multiplet $|1g_{7/2} \otimes 2^+>$ should lie around 1.26 MeV in ^{111}Sn (the 2^+ state in ^{112}Sn being at 1.26 MeV), with strong enhancement in the (^{3}He,α) reaction of the $7/2^+$ member of this multiplet ; we therefore suggest that the new state at 1280 keV could possibly be the $7/2^+$ member of this multiplet. The second multiplet $|2d_{5/2} \otimes 2^+>$ is expected around 1.41 MeV, with preferential enhan-

cement of the $9/2^+$ member, as was observed in the ^{115}Sn case. We therefore tentatively assign $J^\pi=9/2^+$ to the 1470 keV state. Our proposed $J^\pi=7/2^+$ and $9/2^+$ for the levels at 1280 and 1470 keV are compatible with values of $(5/2,7/2,9/2)^+$ proposed by Madueme in his γ-decay work[12] and in agreement with two-step DWBA calculations of the recent (p,d) work[20].

Negative parity levels, based on the coupling between the 3^- state in ^{112}Sn (at $E_x = 2.35$ MeV) and the $1g_{7/2}$ and $2d_{5/2}$ hole configurations are expected around ~ 2.4 MeV in ^{111}Sn. In addition, the $|1h_{11/2} \otimes 2^+>$ multiplet is also expected in the same energy region i.e. $\sim$ 2.24 MeV. Thus, negative parity states should dominate above $\sim$ 2 MeV in the ^{111}Sn spectrum and the strong and complex structures observed at 2070 and 2320 keV probably include, as in ^{115}Sn, levels corresponding to $\ell=5$ $(11/2^-)$ and $\ell=3$ $(5/2^-,7/2^-)$ transitions. This assumption is in good agreement with the proposal by Madueme[12] of a level at 2060 keV with $J \geq 7/2$, negative parity.

^{119}Sn. In this isotope the $1g_{7/2}$ and $2d_{5/2}$ orbitals are usually assumed to be quite full. The corresponding $7/2^+_1$ and $5/2^+_1$ states lie above 750 keV, in a region where weak coupling states are known to appear (the one phonon 2^+ state lies at 1.17 MeV in ^{120}Sn and the two members of the $|3s_{1/2} \otimes 2^+>$ multiplet have been observed around 920 keV). A fragmentation of these orbitals is therefore expected while in ^{111}Sn the $7/2^+_1$ and $5/2^+_1$ are the two first excited states, with rather pure hole character. The fragmentation of the $2d_{5/2}$ orbital is well established, the strength being appreciably split between at least two known[4,16,19] $J^\pi=5/2^+$ levels at 1090 and 1355 keV, while in ^{115}Sn the $5/2^+_1$ level still concentrates most of the strength. In the case of the $1g_{7/2}$ orbital and of the $7/2^+_1$ level (at 788 keV in ^{119}Sn), we emphasize the drastic decrease of the strength of this component as A increases, observed in our work between ^{115}Sn and ^{119}Sn and in the work of Flemming[4]

between ^{115}Sn and ^{123}Sn. The $5/2^+_1$ and $7/2^+_1$ trends are reproduced by the weak coupling calculations.

We wish to point out that the peak observed at 1355 keV in our experiment is obviously a doublet showing evidence, besides the known 1355 keV ($5/2^+$) level, for a new state at $\sim$ 1385 keV. The rather strong population of this state in the (^{3}He,α) reaction indicates the presence of a transition with $\ell > 2$. It could possibly be the ℓ=4 transition corresponding to the population of the $7/2^+$ member of the $|2d_{3/2} \otimes 2^+>$ multiplet : this $7/2^+$ level has been observed from ^{123}Sn to ^{129}Sn in radioactivity work by Fogelberg et al.[21] and it has a much stronger calculated one hole component in ^{119}Sn ($C_j 0^+$=0.41) than in ^{111}Sn and ^{115}Sn, where it is almost purely collective ($C_j 0^+ \sim 0.04$).

It is clear that higher resolution data and complete angular distributions are needed for ^{111}Sn and ^{119}Sn (and other Sn isotopes) in order to further test the weak coupling model in the intermediate excitation energy range, seldom investigated up to now.

V. Inner hole states in ^{111,115,119}Sn. Fragmentation of the $1g_{9/2}$ strength.

As discussed above, very little hole strength is expected beyond 3.5 MeV excitation energy for the valence hole orbitals ($d_{5/2}$,$d_{3/2}$,$g_{7/2}$,$h_{11/2}$). Therefore the strong structures observed around 4.2, 5.4 and 5.6 MeV in the residual spectra of ^{111}Sn, ^{115}Sn and ^{119}Sn (see Fig.3a,b,c) have been previously[1,3,5,6] attributed to neutron pick-up from the next inner orbital i.e. the $1g_{9/2}$ orbital.

These structures (refered to in the following as "bump B") are clearly fragmented in rather well separated peaks, or groups, in ^{111}Sn and ^{115}Sn and to a lesser extent in ^{119}Sn. The fine structure first reported[1] for the

$1g_{9/2}$ hole orbital in ^{115}Sn is clearly confirmed and even enhanced in this (^{3}He,α) experiment, as shown in Fig.8. A detailed comparison of the fine structure, in the 3 Sn isotopes studied in the present work, is presented in Fig.9. On both sides of the main structure (B), at smaller (region A) and higher (region C) excitation energies, weaker groups are also observed. Above 5.2, 6.5 and 7.0 MeV excitation energies, the ^{111,115,119}Sn spectra no longer present noticeable fine structure, but rather broad and weak structures (around 9 MeV in ^{115,119}Sn) and slowly decreasing cross section (see Fig.3a,b,c). A flat continuous background is finally observed in the energy range of the analog states ($E_x \gtrsim 10$ MeV).

In order to carry out a detailed analysis of the structures observed in the 3 isotopes, the "fine structure" part of the residual spectra was divided into adjacent slices chosen after a careful comparison of the behaviour of the spectra at all angles. The main part of the bump B has limits which are consistent with the ones chosen by Van der Werf et al.[3] in their study of the (d,t) reaction on the tin isotopes and correspond to the narrow ℓ=4 part of the observed structures. All the deduced cross sections were determined after substraction of a continuous background (as defined in Fig.3a,b,c and Fig.9) which smoothly connects the flat part at high excitation energies to the minima of the cross section observed at all angles in the lower energy range (i.e. 3-3.5 MeV). In the absence of any prediction for the background shape and magnitude, the adopted procedure seems to be the most consistent one in order to extract the peaks or structures cross sections. One can notice in Fig.9 that the region A, corresponding to strong discrete peaks in ^{111}Sn and to some weaker states in the two other isotopes, is observed above a rising background. The upper, decreasing part of the bump (region C), does not contain narrow states or groups in ^{119}Sn and was not considered in the analysis of this isotope.

A. ℓ identification.

Typical angular distributions of different slices of the ^{115}Sn spectrum are presented in Fig.10 together with the corresponding DWBA curves. The ratio R of the cross sections at 4° and 12° lab. angles are given for the three Sn isotopes in Table VI.

In ^{115}Sn, the main features of these results are the following

The angular distributions of the peaks in region B are all very similar and are individually best fitted by the ℓ=4 DWBA prediction. The whole region B is nicely reproduced by an ℓ=4 transfer as shown in Fig.10. The strongest peaks previously observed in the (d,t) experiment also corresponded to an ℓ=4 transfer, but some groups in the same excitation energy range were also populated through an ℓ=1 transfer. It is clear from Fig.8 that the angular momentum matching in the (^{3}He,α) reaction, near 5 MeV excitation energy in ^{115}Sn, strongly enhances the ℓ=4 as compared to the ℓ=1 transition. This leads to a more reliable determination of the ℓ=4 strength in the main structure, as compared to previous (d,t) or (p,d) studies.

Region A exhibits also rather pure ℓ=4 states, while around 4.5 MeV, contributions of levels with ℓ=1 transfer are observed. Additionnal ℓ=4 strength is observed in region C, but almost all the levels or groups of levels have their angular distributions obviously modified by ℓ=1 contributions (see Table VI). Such ℓ=1 strength around 4.2 and 6.2 MeV in ^{115}Sn is in overall agreement with the previous works[3].

In the excitation energy range above region C, the angular distributions of slices around 7.5, 8.5 and 11 MeV are reported in Fig.10. The rising shapes at forward angles demonstrate the population of ℓ=1 components. This evidence is especially clear at 11 MeV. At this excitation energy, the matching condition for an ℓ=1 transfer becomes reasonnably fulfilled. We would like

to point out the large spreading of the ℓ=1 components (4 MeV < E_x < 11 MeV) in ^{115}Sn.

Turning now to the ^{111}Sn and ^{119}Sn results, one can notice the rather small and constant ratio R in the whole region B (see Table VI). These results, compared to those obtained for ^{115}Sn, suggest the population of ℓ=4 components, in agreement with previous works[3,5,6]. In ^{111}Sn, the new group of levels observed in region A seems also to have pure ℓ=4 character and carries an appreciable amount of the $1g_{9/2}$ hole strength. The region C exhibits a number of narrow states in ^{111}Sn whereas in ^{119}Sn almost no fine structure is observed in the tail of the main structure B.

B. Fragmentation and observed strength of the $1g_{9/2}$ inner hole.

The spectroscopic factors for each individual peak or group of peaks observed in the "fine structure" energy range (regions A, B and C) for ^{111}Sn, ^{115}Sn and ^{119}Sn are reported in Table VI. The mean excitation energy, width and total spectroscopic strength of the main structures are summarized in Table VII. We would like to emphasize the following points :

- The most striking result is the observation in the three isotopes of a limited number of narrow peaks which have an ℓ=4 angular distribution. It is also interesting to notice the evolution of the fine structure with the mass number, leading to very small peaks superimposed on a wider bump in ^{119}Sn (see Fig.9).

- The narrowest part of the bump (region B), as deduced from this analysis, accounts for about 25% of the $1g_{9/2}$ sum rule limit in the three isotopes. This result, and also the deduced widths, agree with those of Ref.3 for ^{115,119}Sn. In the case of ^{111}Sn, some discrepancies are observed between the present results and those of Ref.3. In that study of the (d,t) reaction

region A was not separated from the main structure, but the total strength observed in regions A+B was only 25% as compared to the 38% measured in the (^{3}He,α) reaction in the same energy interval ; the deduced widths in the two experiments are not consistent (see Table VII). We do not observe the minimum in the width of the main bump for ^{115}Sn. This minimum, attributed to subshell closure, is certainly not very pronounced and remains a puzzling problem.

- The total strengths, measured for the whole A+B+C region, decrease from 62% to 43% and 28% from ^{111}Sn to ^{115}Sn and ^{119}Sn. These figures might be increased by choosing a different background but will, in any case, remain rather low as compared to the sum rule limit. Part of the missing strength seems, according to the present experiment (see Fig.10), somewhat spread up to rather high excitation energy ($\sim$ 10 MeV), in agreement with (^{3}He,α) experiments[6,7] at high energy ($E \gtrsim 100$ MeV) on Sn isotopes. These last experiments give rather large ℓ=4 or 3 contributions up to 8 - 11 MeV excitation energy. Further experiments are needed to settle this point.

It is worthwhile to recall that standard DWBA analysis may not be well suited for highly fragmented hole states. The use of a standard form factor may be questionnable but, in addition, other effects may also play a role. For example, if large collective components exist in the wave functions, preliminary estimates of two step effects indicate small corrections of the main structure strength, but rather large effects (50% to 100%) in the high energy tail of the strength distribution.

C. Discussion.

The observed fragmentation in the three isotopes are compared in Fig. 11 with the predictions of Koeling and Iachello[17]. According to these authors the $1g_{9/2}$ inner hole strength is first fragmented over the collective 3 Q.P

and 5 Q.P states (1 phonon - 1 Q.P and 2 phonons - 1 Q.P states). An additional spreading results from the small mixing of these collective states with the many close-lying non-collective 3 Q.P and 5 Q.P states : the combined fragmentation and spreading widths are predicted to increase from ^{111}Sn to ^{119}Sn, in agreement with the present experimental trend for the main structure B (see Table VII). The theoretical strengths are, however, much larger than the experimental ones and the strong fragmentation observed is not at all reproduced.

A very recent report by Vdovin et al.[22] gives somewhat different predictions for the $1g_{9/2}$ strength. In a 1 MeV energy interval around the main structure, in ^{111,115,119,121}Sn, these authors obtain 49% to 43% of the strength and typically 45% for ^{115}Sn as compared to 75% in Ref.17 and to 25% experimentally observed. This strength decreases from A = 111 to A = 119 in agreement with experiment where, however, this effect is much more pronounced. The improved agreement with experiment is attributed to the following features : first the calculation includes $\lambda > 3$ phonons in addition to the quadrupole (2^+) and octupole (3^-) vibrations, which nevertheless play a major role in the fragmentation. Second, the quasi-particle-phonon interaction strengths and the level density are somewhat larger. This increases both the strengths of the 1 phonon - Q.P fragments (the doorway states) and the spreading by coupling with complicated states. Anyway, none of the two calculations[17,22] is able to reproduce the strong fragmentation revealed in the observed fine structure.

In Ref.22, the spreading is described by a phenomenological spreading width Δ (500 keV) which seems too large, taking into account the experimental results, at least for ^{111}Sn, as shown in Table VII. In this nucleus (and partly in ^{115}Sn), the fragmentation into two or three main groups of strong peaks is the main feature. According to Nomura[23], such groups of peaks

as observed in ^{111,115}Sn(^{119}Sn) on the low energy side of the main $1g_{9/2}$ structure may be related to coupling effects with proton core polarized states. Anyway, in spite of the uncertainties in the experimentally deduced absolute spectroscopic factors, it seems that a significant part of the strength may lie at higher excitation energies, up to 9 - 11 MeV. It would be interesting to consider in particular the coupling with the octupole resonance (LEOR) recently observed in even-even Sn isotopes near 6.2 MeV excitation energy[24] with a strength leading for example in ^{115}Sn to the same β value as the one observed for the 3^-_1 state.

VI. Neutron pick-up to analog states in ^{111,115,119}Sn.

The neutron pick-up reaction is well known to excite[25] in the residual nuclei, both $T_<$ and $T_>$ components of an isospin doublet. Until recently the available data on hole-analog states were limited to a large extent to $T_>$ states in medium weigth nuclei. However, the advent of high energy beams associated with sufficient energy resolution in the exit channel have allowed the investigation of such narrow levels in heavy nuclei[3,5,7,10,26,27] and some very recent results have been obtained on hole-analog states[28-30] in ^{143}Sm and ^{207}Pb. In spite of a severe reduction of the hole strength, due to the isospin factor ($1/2\ T_>$), narrow states are still observable in transfer reactions at high excitation energies (10 to 20 MeV) above a continuous background.

These structures are of importance because they involve many aspects of nuclear structure and reactions (i.e. Coulomb displacement energy, total widths and mixing of the "doorway" states with the surrounding $T_<$ levels, spectroscopic strengths and DWBA analysis of "deeply bound" states, etc.).

A simple calculation of Coulomb displacement energy shows that the ground state analogs in ^{111,115,119}Sn should appear around 10.4, 13.3 and

15.0 MeV excitation energy, respectively. The observed α spectra in the excitation energy range of interest are presented in Fig.12 for the three isotopes. In each residual nucleus one clearly observes a number of sharp levels standing above the continuum. These levels have both correct spacings and relative cross sections with respect to the excitation energies, angular momentum transfer and spectroscopic factors of their parent states in the In isotopes[31-33]. The first three analog states in ^{115}Sn and ^{119}Sn had been previously reported[3,5] in (p,d) and (d,t) reactions on ^{116,120}Sn. Three new analog states in ^{115}Sn, two new in ^{119}Sn and the first four, previously unknown, analog states in ^{111}Sn have been observed in the present work.

These levels are located well above the proton, neutron and α thresholds (for example $S_p = 8.73$ MeV, $S_n = 7.53$ MeV, $S_\alpha = 3.20$ MeV in ^{115}Sn) and their total intrinsic widths Γ have been extracted from the measured peak shapes by unfolding the experimental resolution (identified with the one obtained for bound states). Due to our finite resolution (38 keV) this procedure limits the accuracy of Γ to 10 - 15 keV. The excitation energies and total widths for all the analog states observed are reported in Table VIII.

Recently Bechetti et al.[34] have measured the total width of analog states in Sb and I isotopes by means of the (^{3}He,t) reaction. The values obtained by these authors, in a very close mass region of the periodic table, are in good agreement with the ones listed in Table VIII for the Sn isotopes. A very recent high resolution study of the (p,d) reaction on the Sn isotopes[35] leads to comparable results for the measured widths of the $1g_{9/2}$, $2p_{3/2}$ and $2p_{1/2}$, $T_>$ states.

In order to obtain spectroscopic information on the $T_>$ states in the Sn isotopes, angular distributions have been measured for the 6 analog states in ^{115}Sn from 4° to 22° lab. angles. Only two angles (4° and 12°) have been

recorded in the case of ^{111}Sn and ^{119}Sn. The experimental results were compared to DWBA predictions using the parameters listed in Table I and the normalisation constant N=23. For the bound state wave function, the procedure was somewhat different from the one employed for the $T_<$ states. It has already been noticed that the separation energy method (S.E) was questionable[36] for levels with large separation energies ($B_n \gtrsim 20$ MeV) : the corresponding form factors have small amplitudes at the nuclear surface where the DWBA method is expected to be a good approximation. Therefore, in addition to the usual S.E procedure, we have calculated the neutron form factors for the $T_>$ states by solving the Lane coupled-channels equations (C.C) for an isobaric analog pair[37]. An isovector term $4\,U_1(r)\,t\,.\,T/A$ for the coupling strength, with $U_1(r) = -V_1' \, df(x)/dx$ and $x = (1 + \exp(r - r_o A^{1/3}/a))^{-1}$, was used in the calculations. The term V_1' (116 MeV) is related to the usual isospin coupling strength $V_1 = 25$ MeV [38] by the expression $V_1 = 2\,a\,V_1'/r_o A^{1/3}$. A modified version of the computer code DNUM[39] was employed to solve the C.C equations.

The results of such calculations are compared to the experimental distributions in Fig.13. One should notice that the shapes of the theoretical curves are not dependent on the method used to compute the neutron form factor. The spectroscopic strengths are presented in Table VIII for the $T_>$ states in the three isotopes, together with the spectroscopic information already known from previous studies[3,5,10,26] or for their parent levels[31-33]. They are compared, in case of ^{115}Sn, to the results of Sekiguchi et al.[5] and Van der Werf et al.[3] and to their parent states proton hole strengths ($C^2S_p = (2T_o+1)\,C^2S_n$, where T_o is the isospin of the target nucleus) deduced from (d,^{3}He) studies[31-33].

The results of this analysis of the $T_>$ states in the Sn isotopes suggest the following comments :

i) The shapes of the angular distributions (see Fig.13) are rather well reproduced by the DWBA calculations. The ℓ=1 transfers are the best fitted by the calculations : at these excitation energies the (^{3}He,α) reaction is well matched for the ℓ=1 transition. The maxima (4° lab.) and minima (12° lab.) are very characteristic of an ℓ=1 transfer. This result has been used to establish rather unambiguously the ℓ=1 character of several analog states in ^{111,119}Sn (see Table VIII), for which only these two points have been measured.

The ℓ=4 angular distributions are also in overall agreement with the data. Only the very forward angle data (4°-7°) are systematically higher than the theoretical predictions (see Fig.13). This could reflect the angular momentum mismatch ($\Delta\ell \sim 3$) expected for such high ℓ transfer. The ratio of the experimental cross sections at 4° and 12° lab. angles is very close to 1 and also very characteristic of an ℓ=4 transfer. This ratio was used in order to assign an ℓ=4 transfer to the E_x = 10.47 MeV level in ^{111}Sn and to the E_x = 14.98 and 16.47 MeV levels in ^{119}Sn (see Table VIII).

ii) As expected from previous analysis on hole-analog states[3,5,10,27,29,30,33,40], the separation energy procedure leads to spectroscopic factors on the average much higher than the corresponding ones for parent levels (see Table VIII). The disagreement is larger for the ℓ=4 than for the ℓ=1 transitions. Additional effect due to angular momentum mismatch, as reflected already by the shape of the angular distributions, could be a possible explanation to these observations. The main argument which demonstrates the failure of the S.E method comes from the fact that the deduced C^2S_n strength is larger than, or equal to, the sum rule limit for the already fragmented $g_{9/2}$ and $p_{1/2}$ components.

These discrepancies are reduced by the use of the C.C approach (see Table VIII). However, as mentioned in previous DWBA analysis of hole analog

states in heavy nuclei[10,26,29,30] a consistent comparison with the parent states spectroscopic strengths can only be made if one uses the proton form factor from the Lane coupled equations to deduce the C^2S_p values. These calculations were performed for the low-lying states in ^{115}In and lead to C^2S_p values lower by about 40-50% than the ones listed in the corresponding column in Table VIII. Under such conditions, the observed discrepancies between $(2T_o+1)\ C^2S_n$ and C^2S_p remain large (50-60%) for the ℓ=4 transitions and within the uncertainties of DWBA calculations (15-25%) for ℓ=1 transitions. Moreover the introduction of the same isospin dependent part in the nuclear potential for the analysis of the $T_<$ states would increase the deduced C^2S_n strengths by about 30-40%, depending on the energy of the final states.

iii) A more definite indication of the limits of the C.C approach in the analysis of the $T_>$ states in heavy nuclei comes from the energy splitting $\Delta E_T = 4(T_o+1/2)\ \langle \ell j | U_1(r) | \ell j \rangle / A$, between the $T_<$ and $T_>$ components of a single hole state. Using as before the surface peaked interaction, $U_1(r)$ corresponding to $V_1' \approx 116$ MeV, leads to values lower than the experimental ones by about 4 MeV ($\Delta E_T \sim 7.8$ MeV for ^{115}Sn). Similar behaviour have been already observed in the case of the splitting of the hole states[10,26,29,30] in $^{89,95}Zr$ and in ^{207}Pb. Using a surface peaked interaction $U_1(r)$ a correct energy splitting could only be obtained with a value $V_1' = 210$ MeV, corresponding to a volume term for the isospin dependent part of the nuclear potential $V_1 = 35$ MeV. This value is in good agreement with the ones deduced from binding energies systematics of hole states in heavy nuclei[41]. We would like to point out, however, that this result is inconsistent with the strength $V_1 = 25$ MeV deduced from elastic scattering and charge exchange reaction analysis[38]. It would also lead to larger discrepancies for the spectroscopic strengths of the low-lying neutron and proton hole states.

In conclusion, a number of new hole analog states have been observed in the Sn isotopes. Their identifications are based on their excitation energies and corresponding Coulomb displacement energies (see Table IX), ℓ transfers and spectroscopic strengths, as compared to their parent states. The detailed DWBA analysis of such deeply bound levels has confirmed the inadequacy of the S.E procedure in reproducing their spectroscopic strengths. The use of the C.C calculations, although leading to a reasonable basic description of such states, cannot explain the energy splitting between the $T_<$ and $T_>$ components for high isospin levels ($T_o \gtrsim 6$). This result can be tentatively explained by our lack of knowledge concerning the actual form and strength of the isospin dependent part in the nuclear potential for heavy nuclei. According to theoretical descriptions of heavy nuclei[43] it should include both volume and surface terms. A systematic study of the influence of a volume term in heavy nuclei should be undertaken in order to clarify this question. Additional effects, due to matching conditions or to contributions to the cross section from the high density of $T_<$ unbound states which are not explicitly included in the reaction mechanism, have also to be considered in the analysis of the strength of the analog pairs in heavy nuclei.

VII. Summary.

The present work, performed with good energy resolution (38 keV) as compared to previous (^{3}He,α) studies, allows the observation of a number of new features for both the valence and the inner hole states in the ^{111,115}Sn and ^{119}Sn isotopes.

In the intermediate excitation energy region, new states or groups of levels with ℓ=4 and ℓ=5 angular momentum transfers have been populated in ^{115}Sn. These levels correspond to the fragmentation of the $1h_{11/2}$ and $1g_{7/2}$

valence orbitals and have been explained in the framework of a weak coupling model. Both the shape and the magnitude of the cross sections for such levels are rather well reproduced by coupled channels reaction calculations, using the wave functions determined from the model. The one-hole components, even small, generally dominate the observed cross sections. This model also accounts for the population of "anomalous" $\ell=6$ transitions corresponding to $J^{\pi}=11/2^{+}$ states with collective character. A satisfactory explanation of the $\ell=3$ $(5/2^{-},7/2^{-})$, $\ell=4$ $(9/2^{+})$ and $\ell=1$ transitions is also obtained if one includes in the calculation the $1g_{9/2}$, 2p and 1f inner hole orbitals located above 4 MeV.

In the two other isotopes, new peaks and structures with large ℓ values ($\ell > 2$) are also evidenced in this work. We would like to point out the striking differences observed in the intermediate energy region ($\sim$ 1 to 3.6 MeV) in these two isotopes. This behaviour reflects, in the framework of the weak coupling scheme, the change of the neutron quasi-hole energies with increasing mass number, while the energies of the collective 2_1^+ and 3_1^- remain comparatively independent of A.

In the $1g_{9/2}$ inner hole region, the experiment has established the existence of "fine structure" in the three isotopes, in agreement with the results of our previous (d,t) study on ^{116}Sn. The modification of the fine structure aspect of this inner hole strength with the mass number is clearly demonstrated. A limited number of strongly excited narrow states around 4.2 MeV in ^{111}Sn are populated, whereas in ^{119}Sn the fine structure is less pronounced and the small peaks are observed on an underlying broad bump. The $(^3He,\alpha)$ reaction leads to a more reliable measurement of the $1g_{9/2}$ strength, since the lower ℓ components (2p) are strongly reduced in the bump region. These $\ell=1$ components, however, appear on each side (A and C) of the main

structure B, which contains pure ℓ=4 states. A very large spreading of the ℓ=1 strength up to $\sim$ 11 MeV is suggested by this experiment.

The measured strength in the fine structure region (A+B+C) is equal to 62%, 43% and 28% of the total strength in the ^{111,115,119}Sn isotopes. No more fine structure is observed above these regions and the cross section decreases smoothly up to the IAS region. The theoretical calculations are able to reproduce neither the observed fragmentation nor the deduced spectroscopic strengths.

The corresponding $T_>$ inner hole components with large isospins ($T_>$ = 13/2, 17/2 and 21/2 in respectively ^{111}Sn, ^{115}Sn and ^{119}Sn) are nicely resolved. The analysis of such $T_>$ components of inner hole states using the Lane's form factor, is compared to the standard S.E procedure. Both calculations reproduce very well the shapes of the experimental angular distributions, but lead to rather different results for the spectroscopic strengths. The Lane coupled channels approach applied in a consistent way to both the parent proton hole and the $T_<$ neutron hole levels reveals a number of contradictory results. The analysis demonstrates that for analog states with large isospin a more refined description of the isospin dependent part of the nuclear potential is needed in order to describe the strength of the parent, analog and $T_<$ states in heavy nuclei.

References

1) G.Berrier-Ronsin, G.Duhamel, E.Gerlic, J.Kalifa, H.Langevin-Joliot, G.Rotbard, M.Vergnes and J.Vernotte, Phys. Letters 67B, 16 (1977)

2) G.Berrier-Ronsin, G.Duhamel, E.Gerlic, J.Kalifa, H.Langevin-Joliot, G.Rotbard, M.Vergnes, J.Vernotte, K.K.Seth and K.Heyde, Nucl. Phys. A282 189 (1977)

3) S.Y.Van der Werf, M.N.Harakeh, L.W.Put, O.Scholten and R.H.Siemssen, Nucl. Phys. A289, 141 (1977) and references therein.

4) D.G.Flemming, Orsay Internal Report IPNO-PhN-78-22

5) M.Sekiguchi, Y.Shida, F.Soga, Y.Hirao and M.Sakai, Nucl. Phys. A278, 231 (1977)

6) M.Tanaka, T.Yamagata, K.Iwamoto, S.Kishimoto, B.Saeki, K.Yuasa, T.Fukuda, I.Miura, K.Okada, M.Inoue and H.Ogata, Phys. Letters 78B, 221 (1978)

7) E.Gerlic, J.Källne, H.Langevin-Joliot, J.Van de Wiele and G.Duhamel, Phys. Letters 57B, 338 (1975)
J.Van de Wiele, E.Gerlic, H.Langevin-Joliot and G.Duhamel, Nucl. Phys. A297, 61 (1978)

8) P.D.Kunz, A distorted wave Born approximation computer program, University of Colorado, unpublished

9) C.M.Perey and F.G.Perey, Nuclear Data Tables 13, 293 (1974)

10) S.Galès, E.Hourani, S.Fortier, H.Laurent, J.M.Maison and J.P.Schapira, Nucl. Phys. A288, 221 (1977)
E.Friedland, M.Goldschmidt, C.A.Wiedner, J.L.C.Ford Jr. and S.T.Thornton, Nucl. Phys. A256, 93 (1976)

11) J.N.Luetzelschwab and J.C.Hafele, Phys. Rev. 180, 1023 (1969)

12) G.Ch.Maduemc, L.Westenberg, L.O.Evardson and M.Migahed, Physica Scripta 12, 189 (1975)

13) D.G.Flemming, F.D.Bechetti and E.R.Flynn, Los Alamos Internal Report LA-UR-79-153

14) K.Heyde and P.J.Brussard, Nucl. Phys. A104, 81 (1967), and references therein

15) K.Heyde, private communication

16) B.L.Cohen, in Nuclear spin parity assignments, ed. N.B.Gove (Academic Press, N.Y., 1966) p.365

17) T.Koeling and F.Iachello, Nucl. Phys. A295, 45 (1978)

18) E.Rost and P.D.Kunz, private communication

19) P.E.Cavanagh, C.F.Coleman, A.G.Hardacre, G.A.Gard and J.F.Turner, Nucl. Phys. A141, 97 (1970)

20) P.J.Blankert, Thesis 1979, Amsterdam University

21) B.Fogelberg, L.E. de Geer, K.Fransson and M. af Ugglas, Z. Physik A276, 381 (1976)

22) A.I.Vdovin, Ch.Stoyanov and Chan Zuy Khuong, J.I.N.R., Dubna, 1978, E4-12012

23) Masao Nomura, Prog. Theor. Phys. 55, 622 (1976)

24) J.M.Moss, D.R.Brown, D.H.Youngblood, C.M.Rozna and J.D.Bronson, Phys. Rev. C18, 741 (1978)

25) J.P.Schiffer in Isospin in Nuclear Physics, ed. by D.H.Wilkinson (North Holland, Amsterdam, 1969) p.665

26) S.Galès, E.Hourani, S.Fortier, H.Laurent, J.M.Maison and J.P.Schapira, Nucl. Phys. A228, 220 (1977)

27) R.L.Kozub and D.H.Youngblood, Phys. Rev. C7, 410 (1973)

28) S.Galès, Y. El Hage, S.Fortier, H.Laurent, J.M.Maison and J.P.Schapira, Phys. Rev. C17, 1308 (1978)

29) S.Galès, G.M.Crawley, D.Weber and B.Zwieglinski, Phys. Rev. Letters 41, 292 (1978)

30) G.Duhamel, G.Perrin, J.Chauvin, M.Buenerd, E.Gerlic, J.Guillot, J.P.Didelez, H.Langevin-Joliot and J.Van de Wiele, Phys. Letters 78B, 213 (1978)

31) M.Conjeaud, S.Harar, E.Thuriere, Nucl. Phys. A129, 10 (1969)

32) W.H.A.Hesselinck, B.R.Kooistra, L.W.Put, R.H.Siemssen and S.Y.Van der Werf, Nucl. Phys. A226, 229 (1974)

33) C.V.Weiffenbach and R.Tickle, Phys. Rev. C3, 1668 (1971)

34) F.D.Bechetti, W.S.Gray, J.Janëcke, E.R.Sugarbaker and R.S.Tickle, Nucl. Phys. A271, 77 (1976)

35) H.Ikegami, T.Yamazaki, S.Morinobu, I.Katayama, M.Fujiwara, Y.Fujita, H.Taketani, M.Adachi, Y.Matsuzaki, M.Mataba and N.Koori, Osaka University Annual Report 1977, p.195

36) R.Stock and T.Tamura, Phys. Letters 22, 304 (1966)

37) A.M.Lane, in Isospin in Nuclear Physics, ed. by D.H.Wilkinson (North Holland, Amsterdam, 1969) p.511

38) C.R.Satchler, in Isospin in Nuclear Physics, ed. by D.H.Wilkinson (North Holland, Amsterdam, 1969) p.391

39) M.Beiner and P.Gara, Comp. Phys. Com. 4, 1 (1972)

40) S.Fortier, N.M.Rao, E.Hourani and S.Galès, Nucl. Phys. A311, 324 (1979)

41) T.Ishimatsu, H.Saito, M.Yambe, T.Awaya and H.Nomura, Nucl. Phys. A246, 21 (1975)

42) J.Janëcke, in Isospin in Nuclear Physics, ed. by D.H.Wilkinson (North Holland, Amsterdam, 1969) p.299

43) C.B.Dover and Nguyen Van Giai, Nucl. Phys. A190, 373 (1972).

Figure captions

Fig.1. The α energy spectrum from the $^{116}Sn(^{3}He,\alpha)^{115}Sn$ reaction at 12° lab. The numbers on the top of the peaks refer to ^{115}Sn levels and are listed in Table II. Two successive exposures at different magnetic fields were necessary in order to observe the complete range of excitation energy. The spectrum shown was obtained by combining two successive spectra accumulated at 12°, which had an overlap in excitation energy of about 200 keV.

Fig.2. The α energy spectra from the $^{112}Sn(^{3}He,\alpha)^{111}Sn$ reaction (top part) and the $^{120}Sn(^{3}He,\alpha)^{119}Sn$ reaction (bottom part). The low-lying levels in $^{111,119}Sn$ are labelled by their excitation energies, spins and parities. Only the excitation energies are reported for levels above $\sim$ 1.2 MeV in both isotopes. The procedure used to obtain these spectra is the same as described in the caption of Fig.1.

Fig.3. a) The α energy spectrum from the $^{112}Sn(^{3}He,\alpha)^{111}Sn$ reaction at 12° lab. The excitation energy range displayed (3.0 to 13 MeV) permits the observation of both $T_<$ and $T_>$ components of inner-hole states in ^{111}Sn. The solid horizontal line going from $\sim$3 to 13 MeV represents our assumption about the background. The limits of the regions A, B and C, where is mostly concentrated the $1g_{9/2}$ inner-hole strength, are indicated by vertical solid lines. In the horizontal scale, the binding energies of a proton (S_p) and of a neutron (S_n) are noted. The procedure indicated in the caption of Fig.1 was used for the eight PSD in order to built the spectrum presented here.

b) Same as a) for the $^{116}Sn(^{3}He,\alpha)^{115}Sn$ reaction ($3.5 \leq E_x \leq 16$ MeV).

c) Same as a) for the $^{120}Sn(^{3}He,\alpha)^{119}Sn$ reaction ($3.5 \leq E_x \leq 16$ MeV).

Fig.4. Angular distributions from the $^{116}Sn(^{3}He,\alpha)^{115}Sn$ reaction to discrete levels with $\ell = 2,3,4,5$ and 6 angular momentum transfers. The curves show the DWBA predictions. Each final state is identified by its excitation energy in ^{115}Sn. Vertical bars are statistical errors.

Fig.5. Angular distributions from the $^{116}Sn(^{3}He,\alpha)^{115}Sn$ reaction for weaker and complex structures observed in the intermediate energy range $1 \leq E_x \leq 3.5$ MeV. The curves are DWBA predictions for different ℓ values. Vertical bars are statistical errors.

Fig.6. Weak coupling calculations for the ^{115}Sn nucleus. The experimental excitation energies, spins, parities and spectroscopic factors are presented and compared to the corresponding theoretical predictions.

Fig.7. Comparison between experimental angular distributions and two step process calculations for some levels in ^{115}Sn. The weak-coupling model wave functions for such levels (with large collective components : see Table IV) were used in the calculation. Each state is labelled by its excitation energy, strongest collective wave function component $|I^{\pi} \otimes n\ell j\rangle$ and proposed spin and parity J^{π}. The comparison with the data is made for pure direct pick-up (DWBA or P.U), pure indirect pick-up (I.P.U) and combination of the two processes (P.U+I.P.U).

Fig.8. Detailed comparison between the "fine structure" of the $1g_{9/2}$ inner hole state in ^{115}Sn as observed in the (d,t) and $(^{3}He,\alpha)$ reactions. One can clearly notice the enhancement of the $\ell=4$ levels in the $(^{3}He,\alpha)$ spectrum, as compared to the (d,t) spectrum. The numbers on top of the peaks or groups refer to the centroid energies or dominant structure position of the adjacent slices used in order to extract the angular distributions of these fragmented and narrow structures. They were consistent with the ones chosen in the (d,t) study. The limits of each slice are indicated.

Fig.9. Comparison of the fragmentation and spreading of the $1g_{9/2}$ inner hole orbital in the $^{111,115,119}Sn$ isotopes (fine structure regions A, B and C). Peaks or groups of peaks are labelled by the centroid energy of the adjacent slices used in the analysis in order to extract the angular distributions and C^2S of these fragmented structures (see Table VI). Typical deduced angular distributions for ^{115}Sn are also presented in Fig.10. The vertical and horizontal solid lines indicate respectively the limits of the "bump" regions (A, B, C, see text sect.V) and the background level used in the analysis of the data. One can clearly notice the broadening of the main structure B when the mass number increases (A=111 to 119). Shaded areas correspond to a mixing of ℓ=4+1 transitions.

Fig.10. Typical angular distributions of peaks or groups of peaks belonging to the "inner neutron hole region" in ^{115}Sn. The angular distribution for each slice or group of slices, labelled by its energy limits or centroid, is compared to one step DWBA calculations assuming ℓ=4, ℓ=4+1 or ℓ=3+1 angular momentum transfers. In the high excitation energy range ($E_x > 6.2$ MeV) indications of ℓ=1, 2p, components are clearly observed. A typical background angular distribution ($5 < E < 13.5$ MeV) is also presented for comparison.

Fig.11. Comparison of the experimental fragmentation of the $1g_{9/2}$ inner hole orbital with the calculations of Koeling and Iachello[17] for the ^{111}Sn, ^{115}Sn and ^{119}Sn isotopes. The size of vertical bars represents the strengths of the $1g_{9/2}$ in the displayed energy range for both the experimental states and the theoretically predicted ones. The dashed curves represent the calculated spreading of the $1g_{9/2}$ inner hole orbital in the Sn isotopes. The vertical bars crossed by an oblique line

indicate the regions where $\ell=l+4$ or $\ell=l+3$ strength has been observed (not pure $\ell=4$ regions). The calculation predicts a splitting of the $1g_{9/2}$ neutron hole strength into two main structures : the weaker one, predicted around 5.1, 6.6 and 6.5 MeV in the $^{111,115,119}Sn$ isotopes, comes from the coupling of the $1g_{9/2}$ hole with the 2_1^+ level of the even-even target nuclei.

Fig.12. The α energy spectra from the $^{112,116,120}Sn(^3He,\alpha)^{111,115,119}Sn$ reactions in the energy range where the $T_>$ components of the 1g and 2p inner hole states are expected. One can notice, besides the strong peaks from ^{12}C and ^{16}O contaminants, a number of strongly excited narrow states. These levels, labelled by their neutron hole configuration, are the analog states of the $1g_{9/2}$, $2p_{3/2}$ and $2p_{1/2}$ low-lying levels in the In isotopes.

Table I

Optical parameters used in the analysis of the $^{112,116,120}Sn(^{3}He,\alpha)^{111,115,119}Sn$ reactions at 39 MeV

	V (MeV)	r (fm)	a (fm)	W (MeV)	r_i (fm)	a_i (fm)	λ	Ref.
^{3}He	176.2	1.24	0.67	32.8	1.38	0.84		a)
α	206	1.41	0.52	25.8	1.41	0.52		b)
n	ajusted	1.25	0.65				25	

a) Ref.11

b) Ref.10

TABLE II $^{116}Sn(^3He,\alpha)^{115}Sn$ - 39 MeV

E_x(d,t)[a] 23 MeV	present work n°=pic	E_x keV	ℓ	$J\pi$[b]	C^2S this work	C^2S [a] (d,t)	E_x(d,t)[a] 23 MeV	present work n°=pic	E_x keV	ℓ	$J\pi$[b]	C^2S this work	C^2S [a] (d,t)
0	0	0	-	$1/2^+$	-	0.7							
500	1	500	2	$3/2^+$	1.2	0.9			(2560)	(1)	$(1/2^-)$	(0.15)	
614	2	614	4	$7/2^+$	7.5	5.9	2593	16	2600*	1 + ≥3	$(1/2^-)$ + $\geq 5/2^-$	(0.32)	0.16
714	3	714	5	$11/2^-$	2.03	1.6			2650				
967	4	987	2	$5/2^+$	4.7	4.0			(2700)				
1280	5	1280	2	$3/2^+$	0.005	0.1	2735	19	2745	(6)	$(13/2^+)$		
1420	6	1420	2	$5/2^+$	0.205	0.074	2805	20	2807*	2 + ≥3	$(5/2)^+$ + $\geq 5/2^-$	(0.05) ⟷	0.05
1639*	7	1635	2	$3/2^+$	0.17	0.13						≤0.1	
1734	8	1734	2	$5/2^+$	0.19	0.15	2855		(2860)	(6)			
-	9	1805	6	$(11/2^+)$	(0.14)	-		21	2890	5	$(11/2^-)$	0.027	
1858	10	1857	4	$7/2^+$	0.2	0.33	2930						
1944	11	1950	5	$(11/2)^-$	0.22	(0.077)	2950*		2950	(2)	$(5/2^+)$	0.04	0.03
1984	-	-	-	$1/2^+$	-	0.14	2980	22	2985	5,(4)	$(11/2^-)$	0.03	
		(1995)	(2)	-	-	-	3000				$(5/2^+)$		0.026
2061*	12	2070*	2 + (3)	$5/2^+,(3/2^+)$ $(5/2^-,7/2^-)$	(0.08) ⟷ (0.1,0.07)	0.08	3060	23	3070*	(4) + 5	$(9/2^+)$ $(11/2^-)$	0.2	0.032
2158	13	2155	4	$(7/2,3/2)^+$	(0.12,0.07)	-	3190	24	3190	5	$(11/2^-)$	0.08	
2208*	14	2208*	2 + (3)	$3/2^+,(5/2^+)$ $(5/2^-,7/2^-)$	(0.13) ⟷ (0.22,0.15)	0.13	3300	25	3290	3	$7/2^-,5/2^-$	0.11,0.16	
								26	3405*	5			
2332	15	2335	3	$5/2^-,7/2^-$	0.19,0.13	(0.1)	3500	27	3490*	5,4	$(11/2^-,9/2^+)$	(0.09,0.1)	(-,0.063)
2355			(2)	$(5/2^+)$	(0.05) ⟷	0.05		28	3590*	4,(5)	$(9/2^+,11/2^-)$	<0.07	
2371	16	2370	4	$(7/2,9/2)^+$	0.26,0.15	0.35							
		2450	(1)				3665		3.67		$(9/2^+)$		
2489	17	2487*	4	$(7/2^+)$	0.11		3690	29		4		0.2	0.17
2520				$(5/2^+)$	-	(0.014)	3710		3.73		$(9/2^+)$		

a) see ref.2 : only the levels having an energy correspondance with those observed in the present ($^3He,\alpha$) work are given in column 1.

* broad peak, possibly a doublet

b) known values or/and values proposed and used in the present DWBA calcu...

⟷ means that C^2S value of (d,t) has been taken as a reference.

Table III

Input parameters for "Qu phonon" code (weak coupling calculations in ^{115}Sn)

	$n\ell$	j	E_{qp} (MeV)	$\overline{V_j^2}$
Valence Shells	3s	1/2	0.050	0.42
	2d	3/2	0.600	0.37
	1g	7/2	0.850	0.89
	1h	11/2	0.900	0.18
	2d	5/2	1.450	0.80
Inner Shells	1g	9/2	6.2	1.0
	2p	3/2	6.5	1.0
	2p	1/2	7.5	1.0
	1f	5/2	8.5	1.0
	1f	7/2	9.5	1.0
$\hbar\omega_2 = 1.27$ MeV ; $\xi_2 = 2.0$				
$\hbar\omega_3 = 2.27$ MeV ; $\xi_3 = 1.0$				

Table IV

$^{116}Sn(^{3}He,\alpha)^{115}Sn$: summary of J^{π} proposed assignments from weak-coupling calculation and two-step process analysis ($\ell \geq 3$)

E_x (experiment) (keV)	ℓ [a] DWBA	Unperturbed multiplet E_x (keV)	J^{π} (proposed)	E_x (model) this work (keV)	Wave functions hole component + collective component
1805	6	$\|2^+ \otimes g7/2\rangle$	$11/2^+$	1824	$0 + 0.91\|2^+ \otimes g7/2\rangle + \ldots$
1857	4	~ 1900	$7/2^+$	1972	$-0.34\|0^+ \otimes g7/2\rangle + 0.77\|2^+ \otimes g7/2\rangle + \ldots$
1950	5	$\|2^+ \otimes h11/2\rangle$	$11/2^-$	2014	$0.27\|0^+ \otimes h11/2\rangle + 0.87\|2^+ \otimes h11/2\rangle + \ldots$
2208	(3)	~ 2000	$(7/2^-)$	1980	$-0.05\|0^+ \otimes f7/2\rangle + 0.94\|2^+ \otimes h11/2\rangle + \ldots$
2070	(3)	$\|3^- \otimes s1/2\rangle$	$(5/2^-)$	2280	$0.05\|0^+ \otimes f5/2\rangle + 0.99\|3^- \otimes s1/2\rangle + \ldots$
2305	3	~ 2270	$7/2^-$	2297	$-0.04\|0^+ \otimes f7/2\rangle + 0.98\|3^- \otimes s1/2\rangle + \ldots$
2155	4	$\|2^+ \otimes d5/2\rangle$	$7/2^+$	2257	$0.14\|0^+ \otimes g7/2\rangle + 0.86\|2^+ \otimes d5/2\rangle + \ldots$
2370	4	~ 2250	$9/2^+$	2125	$-0.13\|0^+ \otimes g9/2\rangle + 0.83\|2^+ \otimes d5/2\rangle + \ldots$
2807	(3)	$\|3^- \otimes g7/2\rangle$ ~ 2800	$(5/2^-)$	2852	$0.07\|0^+ \otimes f5/2\rangle + 0.89\|3^- \otimes g7/2\rangle + \ldots$
3070 [b]	(4)	$\|3^- \otimes h11/2\rangle$ ~ 3000	$9/2^+$	2985	$0.063\|0^+ \otimes g9/2\rangle + 0.95\|3^- \otimes h11/2\rangle + \ldots$
	5	$\|3^- \otimes d5/2\rangle$ ~ 3250	$11/2^-$	~ 3300	$0.08\|0^+ \otimes h11/2\rangle - 0.52\|3^- \otimes d5/2\rangle + \ldots$ or $0.05\|0^+ \otimes h11/2\rangle - 0.4\|3^- \otimes d5/2\rangle + \ldots$ or $0.08\|0^+ \otimes h11/2\rangle - 0.37\|3^- \otimes d5/2\rangle + \ldots$ or .....
3290	3		$7/2^-$	3271	$0.056\|0^+ \otimes g7/2\rangle - 0.84\|3^- \otimes d5/2\rangle + \ldots$

[a] Strongest $\ell \geq 3$ transitions observed in the $(^{3}He,\alpha)$ reaction.

[b] Doublet.

Table V

Spectroscopic factors of the first low-lying levels in $^{111,115,119}Sn$ isotopes.

^{111}Sn						^{115}Sn					^{119}Sn				
E_x keV	ℓ , J^π	C^2S a)	C^2S b)	C^2S c)	C^2S a) (model)	E_x keV	ℓ , J^π	C^2S a)	C^2S b)	C^2S a) (model)	E_x keV	ℓ , J^π	C^2S a)	C^2S b)	C^2S a) (model)
0	$4,7/2^+$	6	5	4.5	5.3	0	$0,1/2^+$	–	1.	0.82	0	$(0,1/2^+)$	–	1.8	1.3
154	$2,5/2^+$	4.2	5.6	4.0	3.82	500	$2,3/2^+$	1.2	1.3	1.37	24	$2,3/2^+$	1.8	2.4	2.0
(254)	$(0,1/2^+)$	–	0.48	0.29	0.20	614	$4,7/2^+$	7.5	6.0	6.04	89	$5,11/2^-$	3.5	4.6	5.0
644	$2,3/2^+$	0.65	0.72	0.54	0.24	714	$5,11/2^-$	2.0	3.6	1.93	788	$4,7/2^+$	6.0	5.3	4.0
(755)	$(2,5/2^+)$	–	–		–	987	$2,5/2^+$	4.7	6.0	3.42	920	$(2,5/2^+)$	(0.16)	0.5	0.06
879	$5,11/2^-$	0.85	–	0.82	1.14						1090	$2,5/2^+$	2.6	4.0	2.5
											1355 } (1385) }	$2,5/2^+$	1.32	1.5	1.24
ΣC^2S		12.2 d)	11.8	10.15	10.7			16.4 d)	17.9	13.6			17.3 d)	20.1	16.1
Maximum Sum Rule :				12					16					20	

a) Present work.

b) Ref.4

c) Ref.20

d) The $1/2^+$ state being mismatched in our experiment, we have added the more reliable C^2S $(1/2^+)$ value of Fleming[4] to our other experimental C^2S.

Table VI

Detailed analysis of the fine structure region in the $^{112,116,120}Sn(^{3}He,\alpha)^{111,115,119}Sn$ reactions

	^{111}Sn				^{115}Sn				^{119}Sn			
	"E_x" [a] (MeV)	R [b]	ℓ	C^2S (1g9/2)	"E_x" [a] (MeV)	R [b]	ℓ	C^2S (1g9/2)	"E_x" [a] (MeV)	R [b]	ℓ	C^2S (1g9/2)
A	3.46	2.3	(4)+1	(~ 0.05)	3.67	1.35	4	0.20	3.89	1.25	4	0.07
	3.62	1.1	4	0.20	3.96	1.3	4	0.15	3.98	1.30	4	0.08
	3.73	1.15	4	0.33	4.04	1.37	4	0.17	4.05	1.35	4	0.06
	3.82 / 3.86	1.0	4	0.63	4.14 / 4.20	1.44	4(+1)	0.23	4.21	1.40	4	0.11
				Σ = 1.21	4.3	1.46	4(+1)	0.11				Σ = 0.32
					4.4	1.35	4	0.15				
B	4.04	1.15	4	0.48	4.51	1.45	4(+1)	0.06	4.47	1.4	4	0.03
	4.17	1.20	4	0.97	4.61	1.7	4+1	0.09	4.66 / 4.80	1.35	4	0.10
	4.27	1.1	4	0.58	4.72 / 4.81	1.6	4+1	0.104	4.90 / 4.95	1.45	4	0.14
	4.33	0.9		0.21				Σ = 1.30	5.05	1.5	4	0.18
	4.44	0.95	4	0.40					5.12	1.4	4	0.15
				Σ = 2.6	4.91	1.38	4	0.12	5.20	1.4	4	0.10
C	4.52	1.05		0.30	5.08	1.34	4	0.20	5.33	1.55	4	0.33
	4.61	1.3	4(+1)	0.35	5.14	1.16	4	0.30	5.48	1.5	4	0.18
	4.68	1.15	4	0.35	5.25							
	4.78	0.75	4	0.25	5.31 / 5.38	1.11	4	1.07	5.6 / 5.71	1.5	4	0.55
	4.88	1.89	1	–	5.50	1.23	4	0.13				
	4.96 / 5.01	1.30 / 1.05	4(+1) / 4	0.15 / 0.2	5.60	1.20	4	0.47	5.82	1.5	4	0.2
	5.05	1.09	4	0.15	5.75	1.50	4(+1)	0.27	5.96 / 6.02	1.6	4(+1)	0.27
	5.14	–		(0.15)				Σ = 2.56				
	5.21 / 5.27	–	(4) / (4)	(0.50)	5.90 / 6.0 / 6.07	1.60	4+1	0.35	6.12 / 6.30 / 6.36 / 6.46	1.75 / 1.90	4+1	~ 0.3
				Σ = 2.40	6.21	1.65	4+1	0.28				Σ = 2.5
					6.47	–	4+1	0.21				
								Σ = 0.84				
	Percentage of the total 1g9/2 strength			62%	Percentage of the total 1g9/2 strength			43% [c]	Percentage of the total 1g9/2 strength			≲ 28%

[a] "E_x" refers to the energy centroid (or energy of the dominant structure) of each of the adjacent slices. It corresponds to the energy given in Figs.8 and 9.

[b] $R = \sigma(4°)/\sigma(12°)$

[c] An estimate of the ℓ=1 contribution has been substracted from the partial sums given above. These partial sums were obtained assuming pure ℓ=4 transfer.

Table VII

Summary of measured strengths and widths for the main part of the fine structure region

	This work					(d,t) [b]				C^2S (other works)			C^2S
	E_x (MeV)	$\overline{E_x}$ (keV)	σ [a] (keV)	FWHM [a] (keV)	C^2S	$\bar{E}$ (MeV)	σ [a] (keV)	FWHM [a] (keV)	C^2S	(d,t)	(p,d)	(^{3}He,α)	Theo [g]
^{111}Sn	(3.4-4.5) A+B	4.07	245	575	3.8	3.95	300	705	2.5		3.3 [d]		6.7
	(4-4.5) B	4.22	130	300	2.6						2.02 [d]		6.7
^{115}Sn	(4.8-5.8) B	5.47	246	580	2.5	5.20	240	560	2.5	1.5 [c]	1.9 [e]	1-2 [e] 1.3 [f]	7.8
^{119}Sn	(4.3-6.5) B	5.61	446	1050	2.5	5.45	470	1100	2.5			2.2 [f]	8.0-9.7

a) $\sigma = (\sum_i C^2S_i (E_i - \bar{E})^2 / \sum_i C^2S_i)^{1/2}$; FWHM = 2.35 σ

b) Ref.3.

c) Ref.1.

d) Ref.20.

e) Ref.5.

f) Ref.6.

g) Ref.17.

Table VIII

Summary of the results of the analysis of the (^{3}He,α) reaction to hole analog states in Sn isotopes

Final nucleus	E_x (IAS) (MeV)	Γ (keV)	$E_x - E_o$ [a] (MeV)	E_x(parent) [b] (MeV)	J^π(parent) [b]	ℓ J^π c)	$(2T_o+1)C^2S_n$ [d] (^{3}He,α) [c] S.E	C.C	(p,d) [e] S.E	C.C	(d,t) [f] S.E	C^2S_p (d,^{3}He) [b] S.E	S.E	S.E
^{115}Sn	13.260±0.015	31±10	0.0	0.0	$9/2^+$	4 $9/2^+$	12.1	8.6	7.7	6.2	7.1	5.7	6.7	7.4
	13.630±0.015	44±10	0.370	0.340	$1/2^-$	1 $1/2^-$	2.2	1.1	2.3	1.4	1.9	1.2	1.5	1.7
	13.890±0.015	44±10	0.630	0.600	$3/2^-$	1 $3/2^-$	2.7	1.4	2.6	1.5	2.4	1.7	1.9	2.0
$T_> = 17/2$	14.33 ±0.020	> 40	1.070	0.93 1.04 1.08	$(5/2)^-$	(3) $(5/2^-)$ or (4) $(9/2)^+$	4.01 3.25	2.0 2.3						0.7
	14.76 ± 0.02	50±15	1.900	1.45 1.47 1.48	$(1/2,3/2)^-$ $9/2^+$	4 $9/2^+$	5.41	3.8					0.3 2.9	0.5 2.4
	14.93 ± 0.025	—	1.660	1.65	$(1/2,3/2)^-$	1 $(3/2)^-$	0.54	0.28					0.4	0.4
^{117}Sn	10.47 ± 0.015	25±10	0.0	0.0	$9/2^+$	(4) $(9/2)^+$	9.8	7.9				5.5		
	11.06 ± 0.020	25±10	0.59	0.54	$1/2^-$	(1) $(1/2)^-$	2.0	1.1				1.5		
$T_> = 13/2$	11.34 ± 0.020	30±10	0.87	0.81	$3/2^-$	(1) $(3/2)^-$	2.2	1.1				2.0		
	11.78 ± 0.020	35±10	1.31			(4) $(9/2)^+$ or (3) $(5/2)^-$	1.50 1.25	1.20 0.73						
^{119}Sn	14.98 ± 0.020	30±10	0.0	0.0	$9/2^+$	(4) $(9/2)^+$	1.2	7.60	7.2	5.5		5.9		6.5
	15.34 ± 0.020	40±15	0.36	0.315	$1/2^-$	(1) $(1/2)^-$	1.5	0.74	1.7	0.98		1.2		1.6
$T_> = 21/2$	15.63 ± 0.020	50±15	0.65	0.610	$3/2^-$	(1) $(3/2)^-$	1.35	0.70	2.0	1.2		2.1		1.4
	16.10 ± 0.030	70±20	1.12	1.050	$(5/2)^+$	(1) $(3/2)^-$	(1.15)	(0.60)						(0.5)
	16.47 ± 0.03		1.49	1.45	$9/2^+$	(4) $(9/2)^+$	(4)	(2.6)						2.90

a) E_o is the excitation energy of the ground-state analog from this work.

b) Excitation energies, spins and parities and spectroscopic strengths for the parent states in In isotopes are taken from Ref.31,32,33.

c) Present work.

d) The C^2S_n values deduced from the analyse of $T_>$ states in Sn isotopes were multiplied by $(2T_o+1)$, where T_o is the isospin of the target ground-state, in order to allow a direct comparison with the spectroscopic strength C^2S_p of their parent states.

e) Ref.5.

f) Ref.3.

Table IX

Coulomb displacement energies for analog states in Sn isotopes

Analog-pair	E_x (IAS) (keV)	E_x(Parent) (keV)	ΔE_c (keV) Exp.	Calc.
$^{115}In - ^{115}Sn$	13260	0	13560±30	
	13630	340	13580±30	
	13890	600	13590±30	13565±40
	14330	1040	13570±30	
	14760	1480	13590±30	
	14930	1670	13540±30	
$^{111}In - ^{111}Sn$	10470	0	13720±30	
	11060	590	13710±30	13735±40
	11340	870	13690±30	
$^{119}In - ^{119}Sn$	14980	0	13425±30	
	15340	315	13470±30	
	15630	610	13465±30	13400±40
	16100	1050	13495±40	
	16470	1450	13465±40	

a) The excitation energies from the parent states in In isotopes are from Ref.31,32,33.

b) The Coulomb displacement energies were calculated using the semi-empirical formula : $\Delta E_c = 1430\ (\bar{Z}/A^{1/3}) - 992$, where $\bar{Z}$ is the average charge of the analog pair.

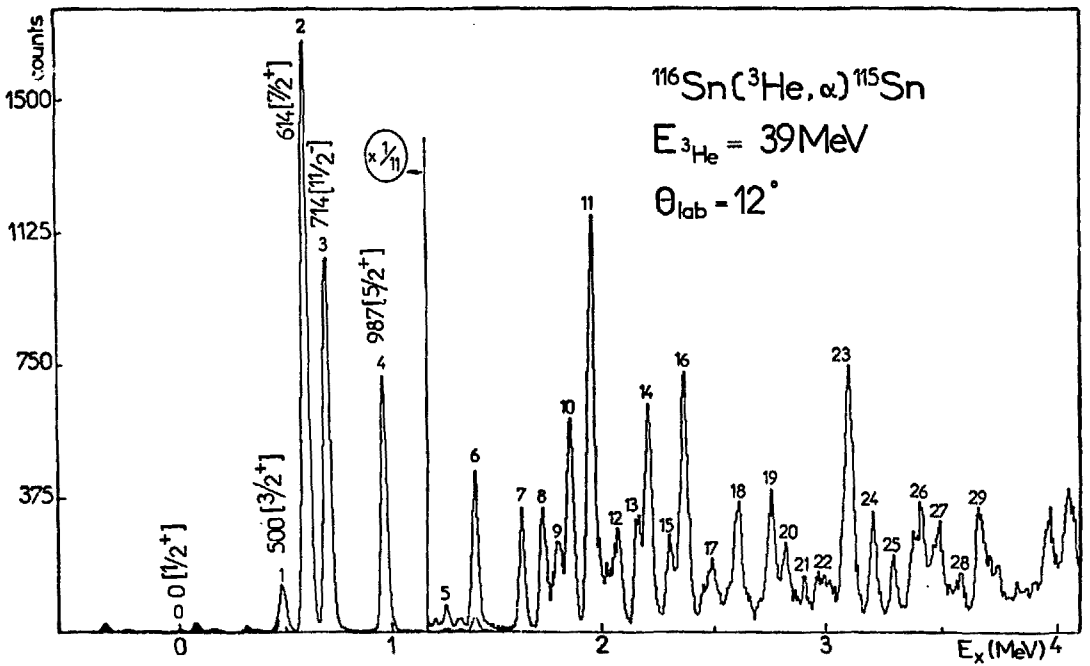
counts
1500
1125
750
375
0
1
2
3
4
E_x (MeV)
$^{116}Sn(^3He,\alpha)^{115}Sn$
$E_{^3He}$ = 39MeV
θ_{lab} - 12°
0 [1/2+]
500 [3/2+]
614 [7/2+]
714 [11/2-]
987 [5/2+]
x 1/11

Fig.1.

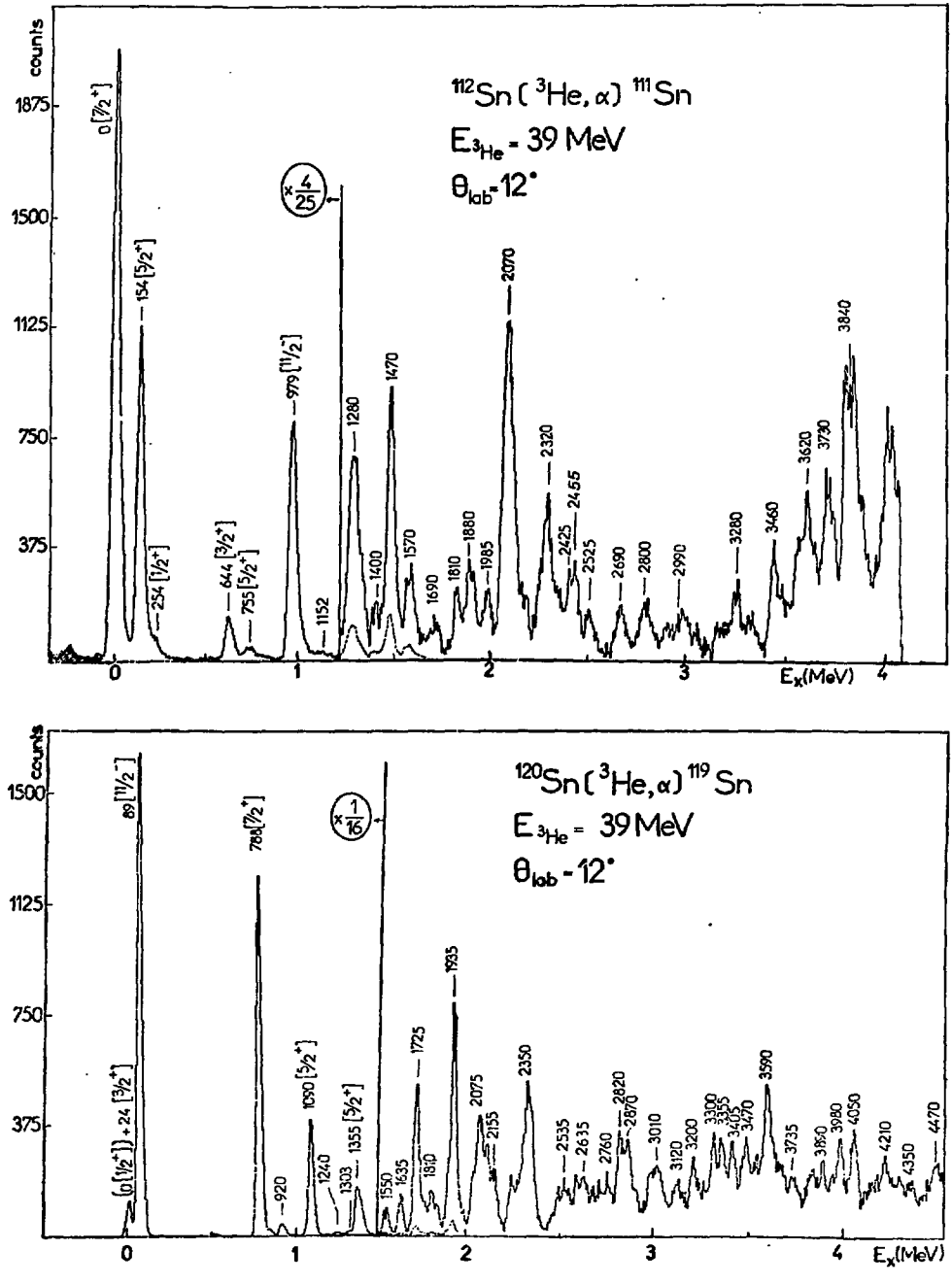
counts
1875
1500
1125
750
375
0
1
2
3
4
E_x(MeV)
^{112}Sn (^{3}He, α) ^{111}Sn
$E_{^3He}$ = 39 MeV
θ_{lab}=12°
× 4/25
0[7/2+]
154[5/2+]
254[1/2+]
644[3/2+]
755[5/2+]
979[11/2-]
1152
1280
1400
1470
1570
1690
1810
1880
1985
2070
2320
2425
2455
2525
2690
2800
2990
3280
3460
3620
3730
3840
^{120}Sn (^{3}He, α) ^{119}Sn
$E_{^3He}$ = 39 MeV
θ_{lab} - 12°
× 1/25
89[11/2-]
(0[1/2+]) + 24[3/2+]
768[7/2+]
920
1090[3/2+]
1240
1303
1355[5/2+]
1550
1635
1810
1725
1935
2075
2155
2350
2535
2635
2760
2820
2870
3010
3120
3200
3300
3355
3405
3470
3590
3735
3850
3980
4050
4210
4350
4470

Fig.2.

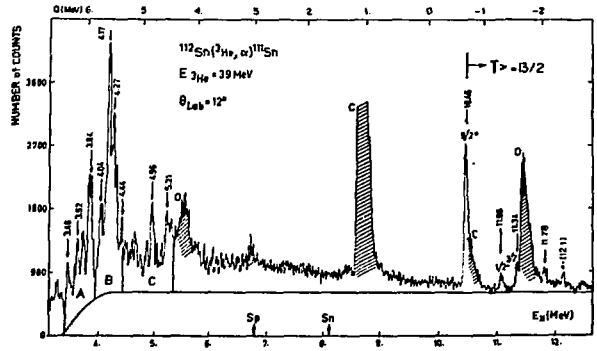

Fig.3.a.

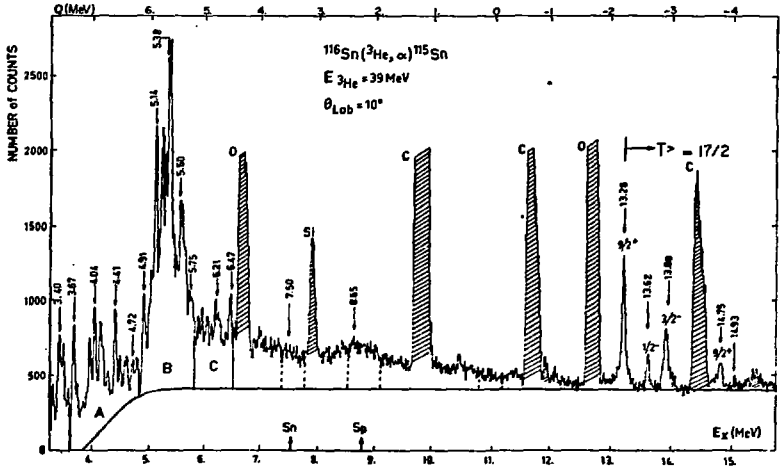

Fig.3.b.

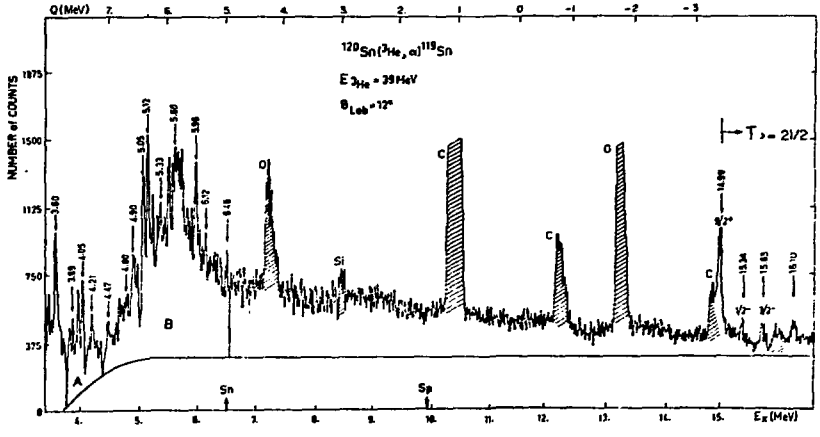

Fig.3.c.

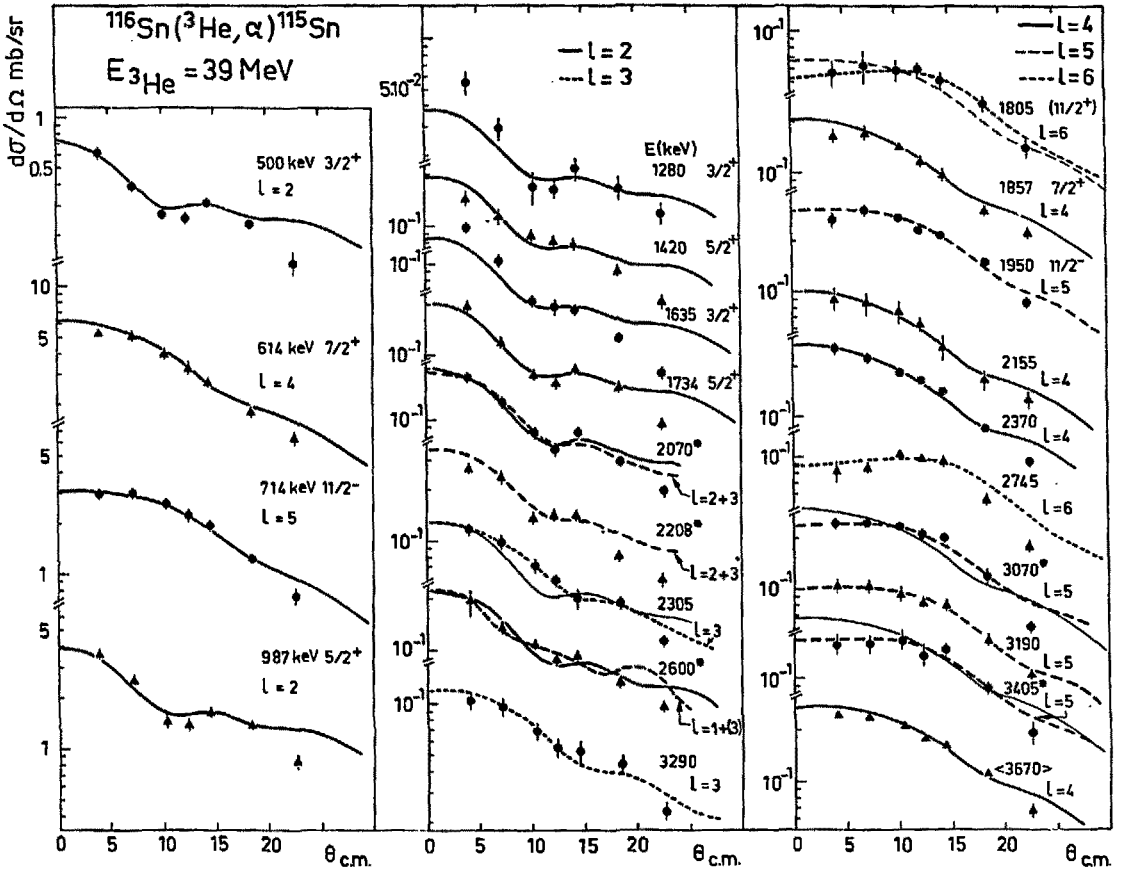
$^{116}Sn(^3He,\alpha)^{115}Sn$
$E_{^3He} = 39$ MeV
dσ/dΩ mb/sr
500 keV 3/2+
l = 2
614 keV 7/2+
l = 4
714 keV 11/2−
l = 5
987 keV 5/2+
l = 2
θ c.m.
l = 2
l = 3
E(keV)
1280 3/2+
1420 5/2+
1635 3/2+
1734 5/2+
2070*
l=2+3
2208*
l=2+3
2305
l=3
2600*
l=1+(3)
3290
l=3
l=4
l=5
l=6
1805 (11/2+)
l=6
1857 7/2+
l=4
1950 11/2−
l=5
2155
l=4
2370
l=4
2745
l=6
3070*
l=5
3190
l=5
3405*
l=5
<3670>
l=4

Fig.4.

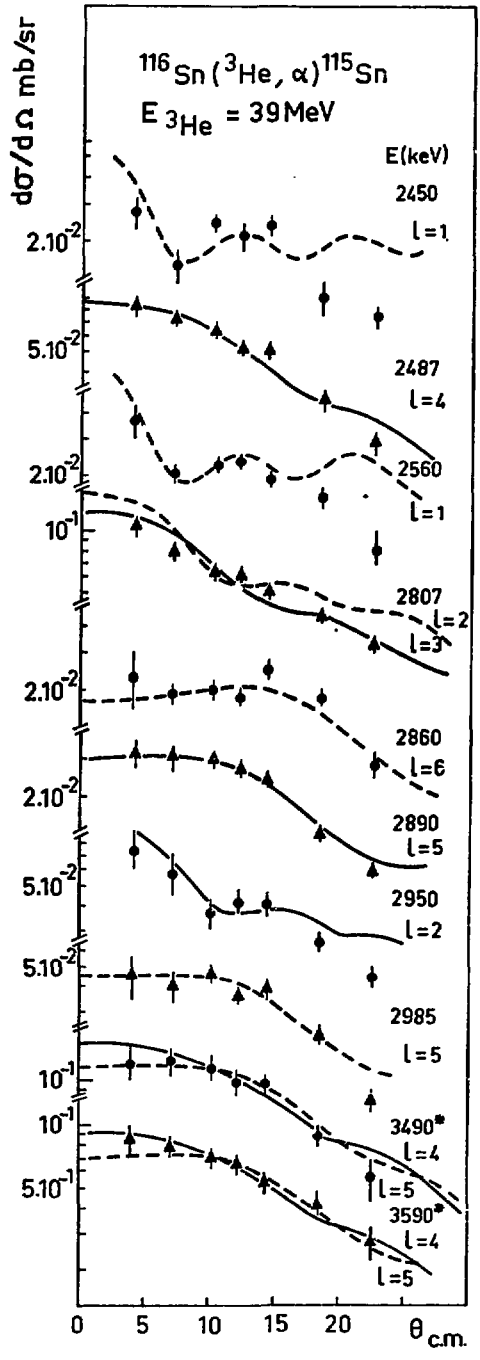
$^{116}Sn(^{3}He,\alpha)^{115}Sn$
$E_{^{3}He}$ = 39 MeV
dσ/dΩ mb/sr
E(keV)
2450
l=1
2487
l=4
2560
l=1
2807
l=2
l=3
2860
l=6
2890
l=5
2950
l=2
2985
l=5
3490*
l=4
l=5
3590*
l=4
l=5
2.10⁻²
5.10⁻²
2.10⁻²
10⁻¹
2.10⁻²
2.10⁻²
5.10⁻²
5.10⁻²
10⁻¹
10⁻¹
5.10⁻¹
0
5
10
15
20
θ c.m.

Fig.5.

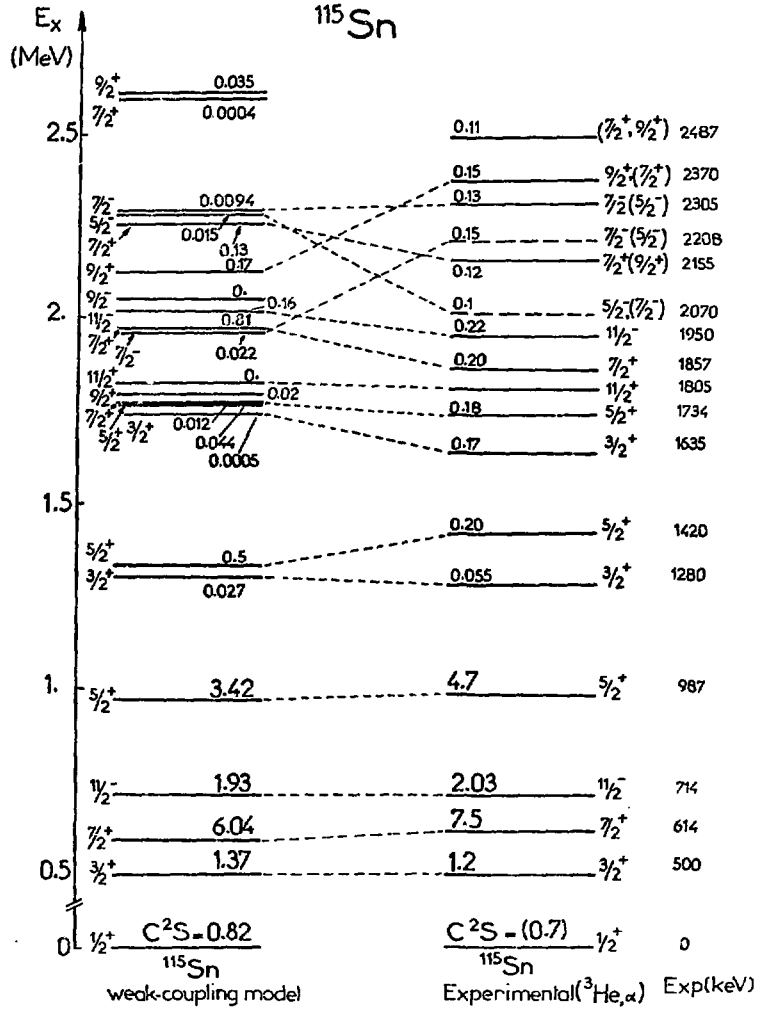
^{115}Sn
E_x (MeV)
2.5
2.
1.5
1.
0.5
0
$9/2^+$ 0.035
$7/2^+$ 0.0004
$7/2^-$ 0.0094
$5/2^-$
$7/2^+$ 0.015 0.13
$9/2^+$ 0.17
$9/2^-$ 0.
$11/2^-$ 0.16 0.81
$7/2^+$ $7/2^-$ 0.022
$11/2^+$ 0.
$9/2^+$ 0.02
$7/2^+$ $5/2^+$ $3/2^+$ 0.012 0.044 0.0005
$5/2^+$ 0.5
$3/2^+$ 0.027
$5/2^+$ 3.42
$11/2^-$ 1.93
$7/2^+$ 6.04
$3/2^+$ 1.37
$1/2^+$ C^2S=0.82
^{115}Sn
weak-coupling model
0.11 $(7/2^+, 9/2^+)$ 2487
0.15 $9/2^+(7/2^+)$ 2370
0.13 $7/2^-(5/2^-)$ 2305
0.15 $7/2^-(5/2^-)$ 2208
0.12 $7/2^+(9/2^+)$ 2155
0.1 $5/2^-(7/2^-)$ 2070
0.22 $11/2^-$ 1950
0.20 $7/2^+$ 1857
$11/2^+$ 1805
0.18 $5/2^+$ 1734
0.17 $3/2^+$ 1635
0.20 $5/2^+$ 1420
0.055 $3/2^+$ 1280
4.7 $5/2^+$ 987
2.03 $11/2^-$ 714
7.5 $7/2^+$ 614
1.2 $3/2^+$ 500
C^2S - (0.7) $1/2^+$ 0
^{115}Sn
Experimental(^{3}He,α)
Exp(keV)

Fig.6.

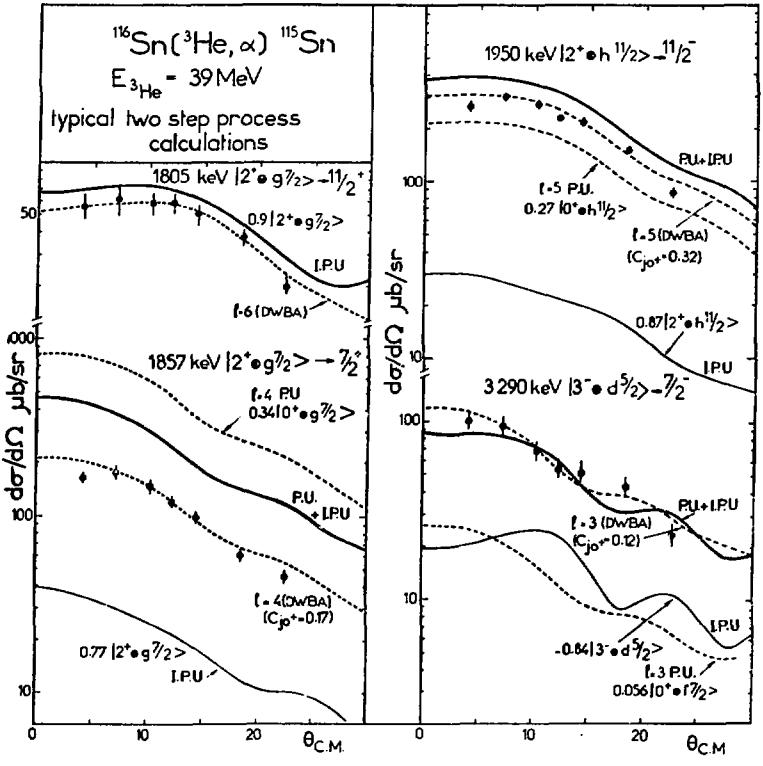
$^{116}Sn(^3He,\alpha)\ ^{115}Sn$
$E_{^3He}$ = 39 MeV
typical two step process calculations
1805 keV $|2^+ \otimes g_{7/2}> \rightarrow 11/2^+$
0.9 $|2^+ \otimes g_{7/2}>$
I.P.U
l=6 (DWBA)
1857 keV $|2^+ \otimes g_{7/2}> \rightarrow 7/2^+$
l=4 P.U
0.34 $|0^+ \otimes g_{7/2}>$
P.U. + I.P.U
l=4 (DWBA)
$(C_{jo^+}=0.17)$
0.77 $|2^+ \otimes g_{7/2}>$
I.P.U
1950 keV $|2^+ \otimes h_{11/2}> \rightarrow 11/2^-$
P.U+I.P.U
l=5 P.U.
0.27 $|0^+ \otimes h_{11/2}>$
l=5 (DWBA)
$(C_{jo^+}=0.32)$
0.87 $|2^+ \otimes h_{11/2}>$
I.P.U
3290 keV $|3^- \otimes d_{5/2}> \rightarrow 7/2^-$
P.U+I.P.U
l=3 (DWBA)
$(C_{jo^+}=0.12)$
I.P.U
$-0.84\,|3^- \otimes d_{5/2}>$
l=3 P.U.
0.056 $|0^+ \otimes f_{7/2}>$
$d\sigma/d\Omega$ μb/sr
$\theta_{C.M.}$

Fig.7.

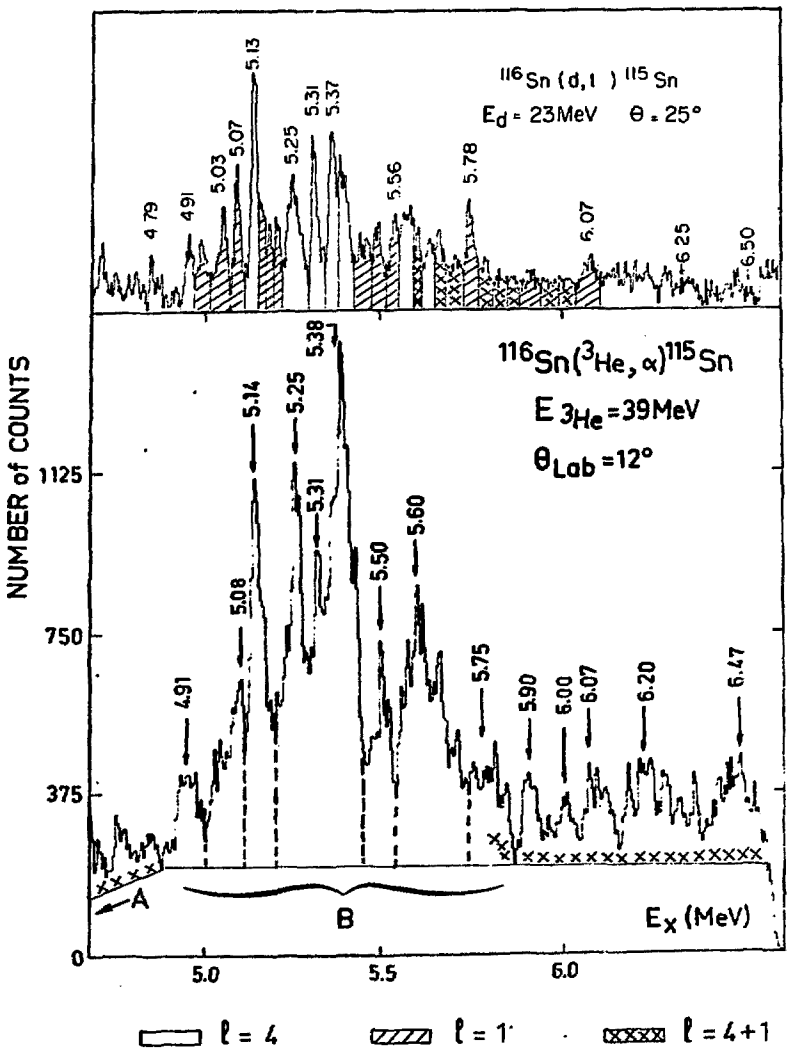
^{116}Sn (d,t) ^{115}Sn
E_d = 23MeV θ = 25°
4.79
4.91
5.03
5.07
5.13
5.25
5.31
5.37
5.56
5.78
6.07
6.25
6.50
^{116}Sn(^{3}He, α)^{115}Sn
$E_{^3He}$ = 39MeV
θ_{Lab} = 12°
NUMBER of COUNTS
1125
750
375
0
5.38
5.14
5.25
5.31
5.50
5.60
5.08
4.91
5.75
5.90
6.00
6.07
6.20
6.47
A
B
E_X (MeV)
5.0
5.5
6.0
ℓ = 4
ℓ = 1
ℓ = 4+1

Fig.8.

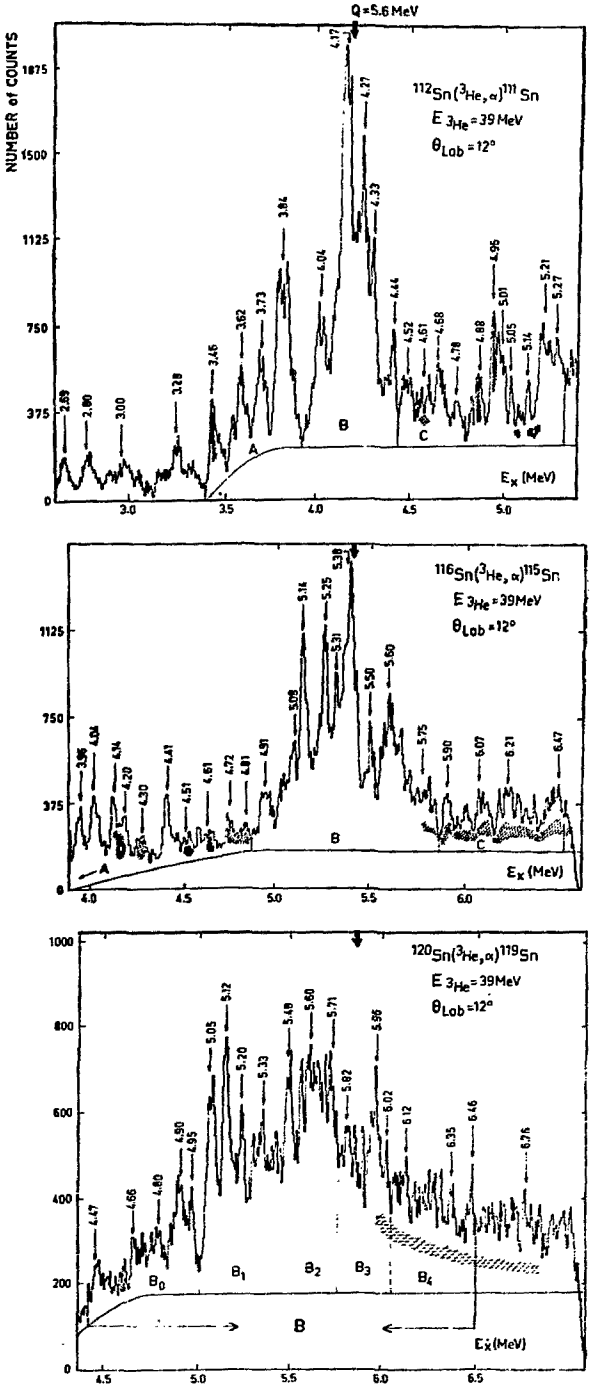
Q=5.6 MeV
NUMBER of COUNTS
$^{112}Sn(^3He,\alpha)^{111}Sn$
$E_{^3He}$=39 MeV
θ_{Lab}=12°
E_x (MeV)
$^{116}Sn(^3He,\alpha)^{115}Sn$
$E_{^3He}$=39MeV
θ_{Lab}=12°
E_x (MeV)
$^{120}Sn(^3He,\alpha)^{119}Sn$
$E_{^3He}$=39MeV
θ_{Lab}=12°
E_x(MeV)

Fig.9.

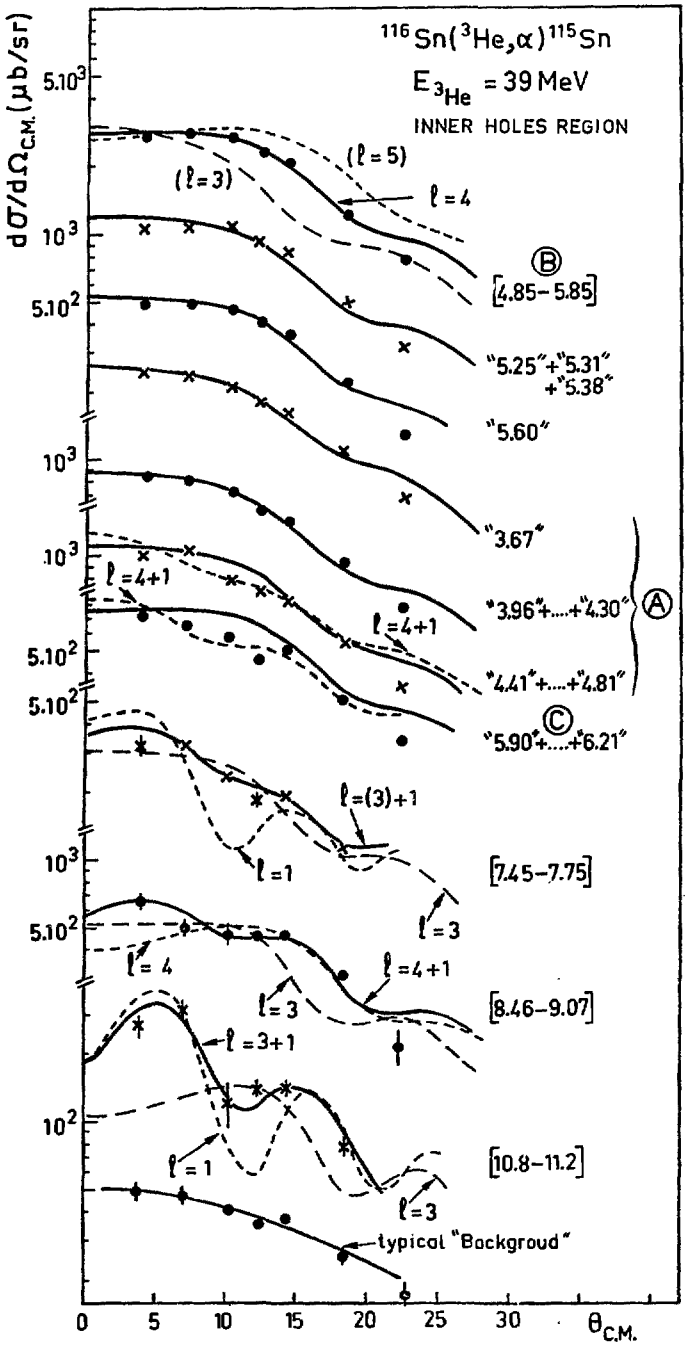
$^{116}Sn(^3He,\alpha)^{115}Sn$
$E_{^3He}$ = 39 MeV
INNER HOLES REGION
$d\sigma/d\Omega_{C.M.}$ (μb/sr)
$\theta_{C.M.}$
(ℓ=5)
(ℓ=3)
ℓ=4
Ⓑ
[4.85–5.85]
"5.25"+"5.31"+"5.38"
"5.60"
"3.67"
ℓ=4+1
"3.96"+....+"4.30"
ℓ=4+1
"4.41"+....+"4.81"
Ⓐ
Ⓒ
"5.90"+....+"6.21"
ℓ=(3)+1
ℓ=1
[7.45–7.75]
ℓ=3
ℓ=4
ℓ=4+1
ℓ=3
[8.46–9.07]
ℓ=3+1
ℓ=1
[10.8–11.2]
ℓ=3
typical "Backgroud"

Fig.10.

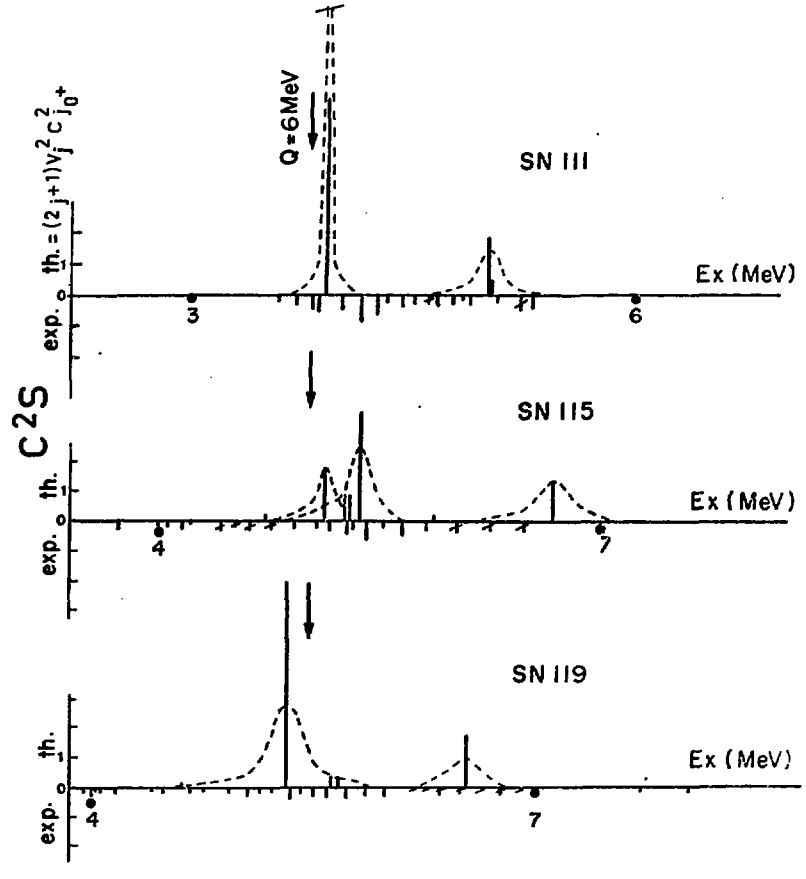
C2S
th.=(2j+1)Vj2C2j0+
exp.
th.
Q=6MeV
SN 111
Ex (MeV)
3
6
SN 115
Ex (MeV)
4
7
SN 119
Ex (MeV)
4
7

Fig.11.

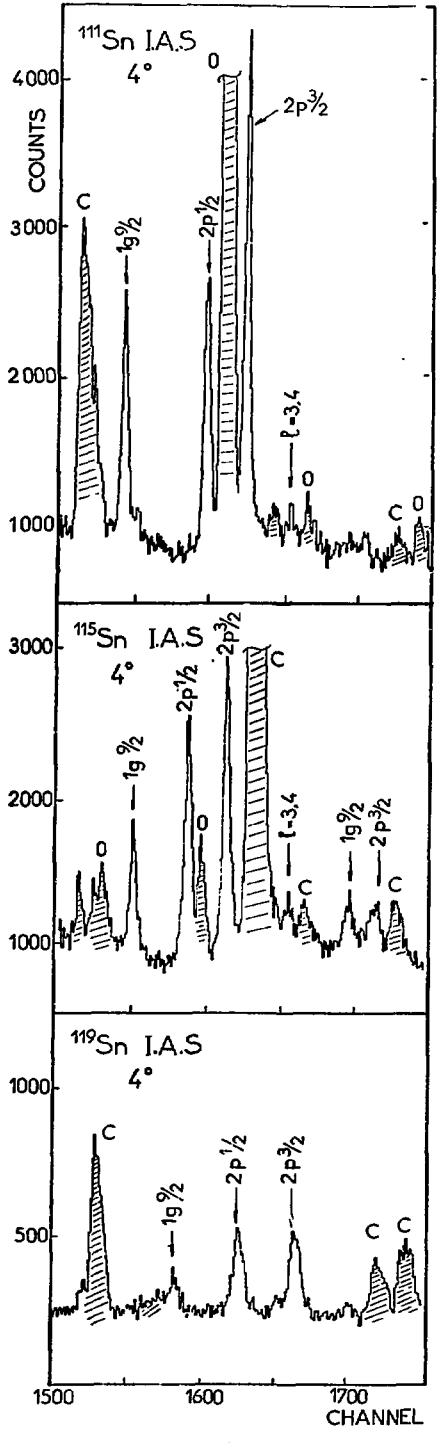
111Sn I.A.S
4°
COUNTS
4000
3000
2000
1000
C
1g9/2
2p1/2
0
2p3/2
ℓ=3.4
0
C
0
115Sn I.A.S
4°
3000
2000
1000
0
1g9/2
2p1/2
0
2p3/2
C
ℓ=3.4
C
1g9/2
2p3/2
C
119Sn I.A.S
4°
1000
500
C
1g9/2
2p1/2
2p3/2
C
C
1500
1600
1700
CHANNEL

Fig.12.

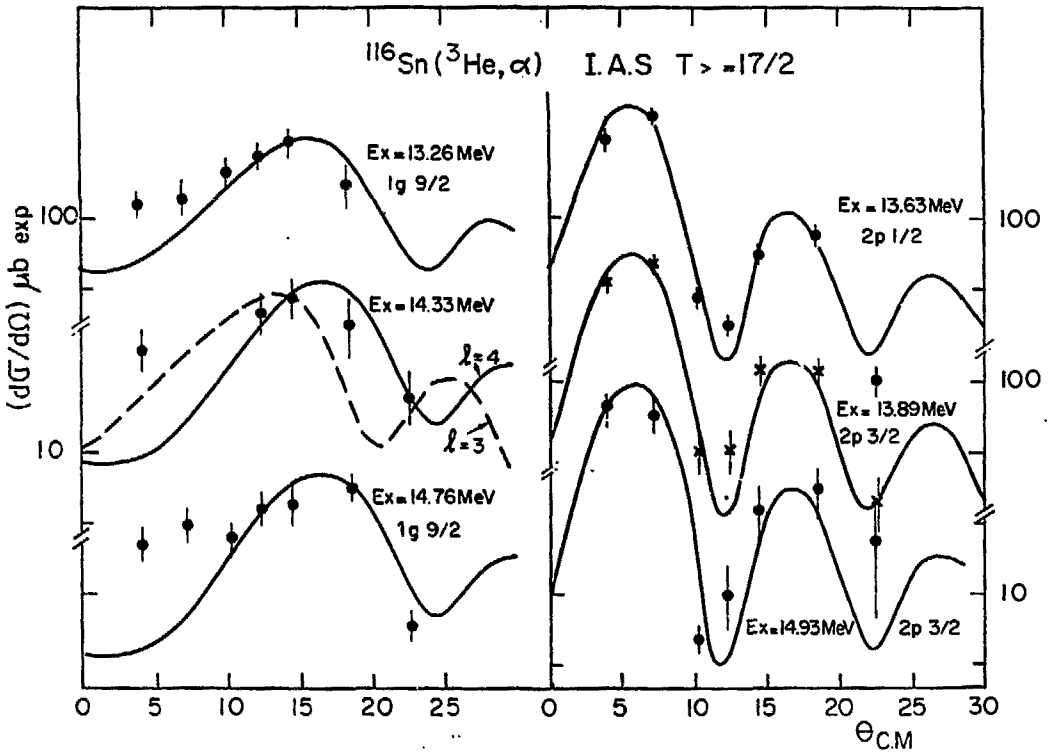
116Sn(3He,α) I.A.S T> =17/2
Ex=13.26MeV
1g 9/2
Ex=14.33MeV
ℓ=4
ℓ=3
Ex=14.76MeV
1g 9/2
Ex = 13.63MeV
2p 1/2
Ex= 13.89MeV
2p 3/2
Ex=14.93MeV
2p 3/2
(dσ/dΩ) μb exp
100
10
100
10
0 5 10 15 20 25
0 5 10 15 20 25 30
ΘC.M

Fig.13.